HIGH ENERGY DENSITY MATERIALS BASED ON FLUORINATED BRIDGED TRINITROMETHYL AZO TRIAZOLE DERIVATIVES: A QUANTUM CHEMICAL STUDY OF THERMODYNAMIC AND ENERGETIC PROPERTIES

Clemence Robinson Ansbert

A Dissertation Submitted in Partial Fulfillment of the Requirements for the Degree of Master's in Materials Science and Engineering of the Nelson Mandela African Institution of Science and Technology

Arusha, Tanzania

March, 2021

ABSTRACT

High energy density materials (HEDM) have gained extensive attention due to their energetic properties and safety issues. Nitro and fluoro groups, among others, have become viable substituents in the HEDM triazole framework because of their particular contribution to detonation properties and moderate sensitivity. In this study, fluorinated bis(trinitromethyl) azo triazoles were designed theoretically using the Density Function Theory (DFT) approach with hybrid functional B3LYP. The molecular structures, thermodynamic properties of gaseous species (e.g., enthalpies of detonation and enthalpies of formation) and energetic properties of solid materials (detonation heat Q, pressure PD and velocity VD) have been investigated. The best characteristics attained for the designed azo fluorinated solid compounds are as follows: Q 1650 – 1690 cal g^{-1}, PD 44 – 46 GPa and VD 9.8 km s^{-1}. These characteristics are superior to those of conventional explosives, indicating that fluorinated bis(trinitromethyl) azo triazoles are promising HEDM.

Keywords: High energy density materials, Fluorinated bis(trinitromethyl) azo triazoles, DFT, Thermodynamic and Energetic properties.

DECLARATION

I, Clemence Robinson Ansbert do hereby declare to the Senate of the Nelson Mandela African Institution of Science and Technology that this dissertation is my original work and that it has neither been submitted nor being concurrently submitted for degree award in any other institution.

Clemence Robinson Ansbert

	11-JUNE-2021
Name and signature of candidate	**Date**

The above declaration is confirmed

Prof. Alexander Pogrebnoi

	11-06-2021
Name and signature of supervisor 1	**Date**

Prof. Tatiana Pogrebnaya

	12/06/2021
Name and signature of supervisor 2	**Date**

COPYRIGHT

This dissertation is copyright material protected under the Berne Convention, the Copyright Act of 1999 and other international and national enactments, in that behalf, on intellectual property. It must not be reproduced by any means, in full or in part, except for short extracts in fair dealing; for researcher private study, critical scholarly review or discourse with an acknowledgement, without a written permission of the Deputy Vice-Chancellor for Academic, Research and Innovation, on behalf of both the author and the Nelson Mandela African Institution of Science and Technology.

CERTIFICATION

The undersigned certifies that they have read and hereby recommend for acceptance by the Nelson Mandela African Institution of Science and Technology a dissertation entitled; "High energy density materials based on fluorinated bridged trinitromethyl azo triazole derivatives: a quantum chemical study of thermodynamic and energetic properties", and recommend for examination in partial fulfillment of the requirements for the degree of Master's in Materials Science and Engineering of the Nelson Mandela African Institution of Science and Technology.

Principal supervisor

Prof. Alexander Pogrebnoi

Signature

11-06-2024

Date

Co-supervisor

Prof. Tatiana Pogrebnaya

Signature

12/06/2024

Date

ACKNOWLEDGEMENT

First, I am thankful to the almighty God, for granting me this gift of life as I am of good health and strong. I wish to express my sincere gratitude to my supervisors; Prof. Alexander Pogrebnoi and Prof. Tatiana Pogrebnaya for their advice, wisdom, assistance, patience, immense knowledge and the highest level of commitment that they have shown to the completion of this dissertation. On top of that, I am indebted to the whole NM-AIST community for their support during the whole time of my study, they were ready to help me whenever I wanted help.

I also extend my sincere thanks to University of Buea, Cameroon for computational facility access. Also special thanks to Mr. Daniel Madulu for providing me the link with university of Buea. Moreover, I would like to expand my grateful appreciation to MEWES School staff who in one way or another provided me with moral support and encouragement; most specifically Prof. Revocatus Machunda and Dr. Mwemezi Rwiza to mention a few.

It would be unfair if I will not give sincere thanks to my fellow students, Mr. Geradius Deogratias, Mr. Rene Costa and Ms. Catherine Paschal from MESE Department for their support and encouragement.

Finally and exceptionally, my special thanks also go to my family members: My parents Mr. and Mrs. Ansbert Kahatano for their support and encouragement as well as my employer Mwenge Catholic University (MWECAU) for granting me study leave. Lastly, may the living God bless you all, amen.

DEDICATION

This work is dedicated to my family, staff mates and friends who have always been there for support throughout my study.

TABLE OF CONTENTS

LIST OF TABLES

LIST OF FIGURES

LIST OF APPENDICES

LIST OF ABBREVIATIONS AND SYMBOLS

B3LYP	Becke, 3-Parameter, Lee–Yang–Parr
RDX	Cyclotrimethylenetrinitramine
A	Degree of Self Oxidation
DFT	Density Function Theory
Q	Detonation Heat
PD	Detonation Pressure
VD	Detonation Velocity
DFDNT	Difluorodinitrotoluene
DFTNT	Difluorotrinitrotoluene
Fox-7	Diminodinitroethene
DNT	Dinitrotoluene
GIPF	Generalized Interact Property Function
CL-20	Hexanitrohexaazaisowurtzitane
HEDM	High Energy Density Materials
HOMO	Highest Occupied Molecular Orbital
$h_{50\%}$	Impact Sensitivity
IR	Infrared Radiation
LUMO	Lowest Unoccupied Molecular Orbital
ρ_{mol}	Molecular Density
OB	Oxygen Balance
PETN	Pentaerythritol Tetranitrate
PFDNT	Pentafluorodinitrotoluene
HMX	Tetranitrotetrazoctane
TDF	Thermodynamic Functions
TNT	Trinitrotoluene
ZPVE	Zero-point Vibration Energy

CHAPTER ONE

INTRODUCTION

1.1 Background of the Problem

Energetic materials belong to a class of materials which contain high amount of deposited chemical energy that can be released (Brinck, 2014). This energy is released by rapid propagation reaction known as detonation reaction (Millar, 2011; Tarver, 2020). In comparison with deflagration and combustion reactions, detonation reaction is speedier and supersonic shock waves (Diegelmann *et al*., 2016). It is also an exothermic reaction which leads to an increase in pressure and temperature of the system (Collins & Gottfried, 2017). Materials of this class include common fuels such as gasoline and diesel (Olah & Squire, 2012) which are used to power automobiles, and explosives such as dynamite, gun-powder and trinitrotoluene (Luan *et al*., 2010).

World high energy materials demand is now increasing and has reached an exceedingly high level (Talawar *et al*., 2009). The economy, political state and population growth of different nations are closely linked to availability of energetic materials products (Talawar *et al*., 2009). The science of high energy density materials is now active because of widespread applications of these materials in defense, exploration and mining of minerals, forecasting earthquakes, construction industry, correcting weather phenomena, extinguishing fires, production of nanomaterials and metals processing (Dalinger *et al*., 2018). Several materials are currently exploited to meet the needs for industrial development through production of strong and reliable instruments for industries (Palysaeva *et al*., 2019).

Almost all traditional energetic compounds such as pentaerythritol tetranitrate (PETN), trinitrotoluene (TNT), cyclotrimethylenetrinitramine (RDX), 2, 4, 6, 8, 10, 12-hexanitrohexaazaisowurtzitane (CL-20) and 1, 3, 5, 7-tetranitro-1, 3, 5, 7-tetrazoctane (HMX) are explosives and therefore environmental unfriendly and are considered to be dangerous (Thottempudi & Shreeve, 2011). Therefore, the scientific community is in the drive to design and prepare novel high energy materials such as energetic polymers, polynitro compounds, energetic salts and nitrogen rich compounds for technological development and energy production (Dharavath *et al*., 2017).

A fashionable approach to the field of energetic materials is to substitute some explosives with high energy groups containing materials. These compounds contain high proportion of high energy groups by mass relative to traditional explosives (Zhang *et al*., 2019). High nitrogen compounds such as azoles together with energetic substituent groups such as nitrato ($-ONO_2$), nitroimine ($=NNO_2$), nitramine ($-NHNO_2$) and nitro ($-NO_2$) functional groups are of particular interest due to their satisfactory oxygen content (Fischer *et al*., 2010; Holl *et al*., 2003; Karaghiosoff *et al*., 2003; Semenov *et al*., 2017; Thottempudi & Shreeve, 2011). These compounds burn more cleanly producing less soot, less carbon monoxide and the major product of explosion is nitrogen gas (Türker, 2016).

Elevated properties; enthalpy of formation, detonation pressure, density, thermal stability, detonation velocity and low sensitivity towards external forces such as friction, shock and impact are the necessary characteristics for energetic materials (Türker, 2016). These properties can be achieved by choosing the number, type and position of the substituent groups in the framework (Dalinger *et al*., 2018). Fluorinated compounds are subject of thorough research due to their exceptional detonation properties (Martinez *et al*., 2012). High fluorine content together with hydrogen results in the formation of hydrogen fluoride upon detonation which generates high amount of energy (Ye *et al*., 2007). The existence of fluoro groups also increases the density of the substance (Dalinger *et al*., 2018; Zhang *et al*., 2019). Fluorinated bis(trinitromethyl) azo triazoles show a promising solution due to ability of fluoro group to enhance energetic nature of the material.

1.2 Statement of the Problem

Majority of high energy materials are highly sensitive towards external impact which makes them environmentally unfriendly. However, some polynitro compounds which are not harmful have been prepared but they show less energetic properties as compared to traditional explosives and others are highly sensitive and concern complex synthesis methods (Zhang *et al*., 2019). So, there is a need to find new energetic materials which are less sensitive and at the same time simpler to synthesize. In order to attain high energetic nature, the group attached to a highly nitrated compound should be highly energetic such that upon detonation, high amount of energy is generated. Therefore, the present study aimed at design of new energetic materials via fluorinating bis(trinitromethyl) azo triazoles towards improving energetic performance.

1.3 Rationale of the Study

Much work has been carried out in the area of high energy density materials by investigation of various azole compounds, but less done on the effect of fluoro substituents on highly nitrated compounds. The improvement of energetic properties has been growing at a slow pace; this is associated with low level of understanding of chemical process such as electron transfer within the material itself. The performance of energetic materials is assessed mostly by considering the amount of released energy, speed of detonation, detonation pressure and type of products formed. Therefore, the present study will help to screen potential compounds with desirable properties to be considered as potential energetic materials.

1.4 Research Objectives

1.4.1 General Objective

To design new energetic materials with higher energy contents by introducing fluoro groups into bis(trinitromethyl) azo triazoles.

1.4.2 Specific Objectives

(i) To design fluoro bis(trinitromethyl) azo triazoles compounds and investigate their geometry, electronic structure and vibrational spectrum.

(ii) To determine the thermodynamic functions, thermal stability and energetic properties of the compounds.

1.5 Research Questions

(i) What are the structural, electronic, vibrational, thermodynamic and energetic properties of fluorobis(trinitromethyl) azo triazoles?

(ii) What are the effects of fluoro substituent groups on the energetic properties of bis(trinitromethyl) azo triazoles?

1.6 Significance of the Study

The knowledge of the geometrical structures, vibrational frequencies, thermodynamic and energetic properties will provide clear direction and understanding of the influence of fluoro and other energetic groups on the properties of bridged and non-bridged azole compounds.

Furthermore, this study will be used as a framework for further theoretical and experimental investigations of new high energy materials.

1.7 Delineation of the Study

The study was conducted theoretically on fluorinated bis(trinitromethyl) triazoles. The molecules were designed and studied using various software as summarized in Table 4. The geometry optimization, HOMO-LUMO orbitals and vibrational frequencies computations of all designed molecules were performed using density functional theory (DFT) with hybrid functional B3LYP and basis set 6-31G(d,p) while thermodynamic characteristics of reactions were obtained with extended 6-311++G(d,p) basis set. The optimized geometrical parameters and vibrational frequencies were used for calculation of thermodynamic functions of the species in the gas and solid phase and the energetic properties. The results were used to predict the performance and stability of the designed compounds.

CHAPTER TWO

LITERATURE REVIEW

2.1 Energetic Materials Properties

Generally, energetic materials are characterized by four basic features (Smirnov *et al*., 2011; Zeman & Jungová, 2016):

(i) They are chemical compounds or mixtures which are ignited by heat, impact, shock, friction or a combination of them.
(ii) They decompose rapidly (detonate) upon ignition.
(iii) Large amount of gases at high pressure is evolved as a result of rapid expansion of those gases with higher forces to overcome confining forces. It is also accompanied by rapid liberation of heat.
(iv) The detonation process accompanied by liberation of energy basically produces four effects; fragmentation, displacement, vibration and air blasting.

Detonation of the material charges results into a high velocity shock wave accompanied by release of gases (Shtertser *et al*., 2020; Walters *et al*., 2020). This wave cracks the rock creating a number of cracks in the rock. The expanding gases produced in the detonation fill up the cracks until its pressure is weak (Bendezu *et al*., 2017; Yuan *et al*., 2019). High energy density materials are characterized by the following parameters as described below.

2.1.1 Density

Density is an important parameter to consider when selecting an energetic material since a denser material is required for easy detonation (Agrawal & Mishra, 2017; Onyelowe *et al*., 2018). It is also important to note that when working under a wet condition, a denser material is necessary. For commercial explosives, the loading density ranges from 0.6 to 1.7 g cm^{-3} (Table 1) (Remennikov *et al*., 2017). Additionally, the density of a free running explosive is expressed depending on the size of a given borehole. It's also worth noting that a denser materials gives higher detonation pressure and velocity with exception of few materials (Mertuszka *et al*., 2018; Mishra *et al*., 2019).

Table 1: Properties of ammonia dynamite (low and high density)

Density level	Weight strength (%)	Density (g cm^{-3})	Confined velocity (km s^{-1})
Low density	65	1.2	2.47
	65	1.1	2.38
	65	1.0	2.29
	65	1.0	2.19
	65	0.9	2.10
	65	0.9	1.98
	65	0.8	1.92
High density	60	1.7	3.81
	50	1.6	3.51
	40	1.5	3.2
	30	1.4	2.74
	20	1.3	2.44

Remennikov *et al*. (2017)

Weight strength is a measure of the energy available in a given weight of an explosive material compared to energy of equal weight of ammonium nitrate fuel oil (ANFO) (Remennikov *et al*., 2017). It is expressed in terms of percent using ANFO as a standard explosive. A weight strength can be absolute or relative. Absolute weight strength, W_A is the ratio of energy available in a given mass of explosive material to an equal mass ANFO, expressed as:

$$W_A = \frac{E_{exp}}{M_{ANFO}} \tag{1}$$

where E_{exp} is the computed energy of an explosive material and M_{ANFO} is the mass of ammonium nitrate fuel oil measured in kilograms.

On the other hand a relative weight strength is the energy per unit mass of an explosive material in relation to that of ANFO. It is expressed using the following equation:

$$E_R = \frac{W_A}{W_{ANFO}} x100\% \tag{2}$$

where W_{ANFO} is the absolute weight strength of ammonium nitrate fuel oil.

2.1.2 Detonation Velocity and Pressure

The velocity of detonation is the measure of the rate at which detonation waves travel in column (confined) or in open space (unconfined) (Jackson, 2017; Poludnenko *et al*., 2019).

Energetic materials in most cases are used in confined spaces. Therefore, it is significant to measure the velocity of detonation in confined spaces (Poludnenko *et al*., 2019; Yunoshev *et al*., 2017). In general, commercial explosives have detonation velocity ranging from 1.52 to 7.62 km s^{-1} (Yunoshev *et al*., 2017). However, the velocity of detonation varies proportionally with the density of the material (Table 1). High velocity material is required for breaking up a hard rock (Kotomin *et al*., 2017). For complete confinement, it is important to consider the diameter of the column since the bigger the diameter, the higher is the velocity.

Pressure of detonation is the principle measure of the materials performance (Keshavarz & Pouretedal, 2004). It relates to the loading density and detonation velocity of the material. A denser rock requires a stronger material in which a high pressure explosive is necessary. Principally, detonation velocity depends on four parameters; heat content of the material, loading density, materials composition and oxygen balance (Keshavarz, 2005).

2.1.3 Impact Sensitivity

Some explosives can easily explode while others not; considering this property, two kinds of explosives are available (Fu *et al*., 2017). Those with higher sensitivity (primary explosive) and others with lower sensitivity (secondary explosives). In general, a typical weight of a sample is dropped in a sequence of tests from a certain height onto the plate and the responses are recorded as $h_{50\%}$ (the value from which 50% of the sample resulted into a reaction) (Cawkwell & Manner, 2019; Kamlet & Short, 1980). The $h_{50\%}$ results can give different values and therefore they are not reproducible (Kamlet & Adolph, 1979). In this regard, the value is a suspect and the clue about the easiest of the materials to be set off by spark, impact, shock, heat and friction (Bowden & Yoffe, 1985; Wilson *et al*., 1990). For 2,4,6-trinitrotoluene, the impact sensitivity vary from 98 cm to 250 cm or above (Wilson *et al*., 1990). The high value of $h_{50\%}$ means that higher dropping height is required for the material to explode and hence the safer the material (Kamlet & Adolph, 1979).

Among others, the impact sensitivity depends on; molecular electronegativities (Mullay, 1987a, 1987b), concentration of detonation gases (Adolph *et al*., 1981; Rice & Hare, 2002), atomic charges (Murray *et al*., 1990; Owens *et al*., 1985), molecular mass (Rice & Hare, 2002), vibrational states (Fried & Ruggiero, 1994; McNesby & Coffey, 1997), detonation enthalpy (Rice *et al*., 2007), enthalpy of formation (Keshavarz *et al*., 2007; Rice *et al*., 2007)

and oxygen balance (indicator of self oxidation of the compound) (He & Shreeve, 2016). Additionally, the sensitivity is highly related to electrostatic potential of the compound which is associated with molecular structure and electronegativity values of the atoms present in a compound (Murray *et al*., 1995). This is caused by building up of localized positive charges over the region of covalent bonding in a molecule (Politzer *et al*., 1982; Sjoberg & Politzer, 1990). For highly nitrated and fluorinated energetic compounds, the localized positive charges build up over C-F, N-F and C-NO_2 bonds causing the increase in sensitivity of the molecule (Politzer *et al*., 1984).

Theoretically, four methods have been developed for the determination of impact sensitivity of energetic materials. These are based on detonation enthalpy and electrostatic potential properties (Rice & Hare, 2002) collectively called Generalized Interact Property Function (GIPF). The four methods are represented by the following equations, respectively:

$$h_{50\%} = 9.2 + 803\exp(-0.0875\,|\bar{V}^{+} - |\,\bar{V}^{-}||) \quad (3)$$

$$h_{50\%} = 29.3 + 0.001386\exp(48.84\upsilon) \quad (4)$$

$$h_{50\%} = 27.8 + 0.1135\exp(-2.6479Q + 18.40) \quad (5)$$

$$h_{50\%} = 1.341\exp(8.1389\upsilon - 1.6234Q + 10.01) \quad (6)$$

where Q is the detonation heat, $\bar{V}^{+}$ is the average value of positive electrostatic potential, $\bar{V}^{-}$ is the average values of negative electrostatic potential and υ is the index of charge balance obtained using Multiwfn program package (Lu & Chen, 2012). All values of $h_{50\%}$ are measured in centimeter.

It has been reported that method 2 (equation 4) provides reliable data which is nearly related to the experimental values for traditional explosives as presented in Table 2.

Table 2: Predicted and experimental values of $h_{50\%}$ (cm) for traditional explosives

Compound	Method 1	Method 2	Method 3	Method 4	Experimental
TNT	73	80	133	143	98
RDX	49	31	39	22	28
HMX	21	31	41	22	32

Mei *et al*. (2019)

2.1.4 Detonation Heat

Heat of detonation, is the total energy evolved during detonation reaction (Tarver, 1982a, 1982b). During detonation, several chemical reactions are taking place step by step. These reactions are exothermic and liberate a certain amount of heat energy collectively called detonation heat, Q (Politzer & Murray, 2015). The amount of heat energy released depends on the speed of the reaction progress; the slower progress, the lower energy will be released and hence few noticeable effects will be observed (Keshavarz & Pouretedal, 2004). On the other hand, higher energy is liberated when the reaction proceeds rapidly with high speed. The chemical explosion reaction involves oxidation in a limited number of simple partial reactions of each atom within a molecule with oxygen in order of preference (Keshavarz, 2008; Schultz & Shepherd, 2000). The preference is in the following order; metal, carbon, hydrogen, carbon monoxide, excess O, H and NO_2. The heat of detonation is computed as the difference between the enthalpies of formation of the compounds before and after detonation (Kamlet & Hurwitz, 1968) as follows:

$$Q = \Sigma \Delta_f H^{o}_{react} - \Sigma \Delta_f H^{o}_{prod} \quad (7)$$

The Q is usually expressed in cal g^{-1} when the result obtained from equation (7) is divided by the molecular weight of the compound (Kamlet & Jacobs, 1968). The value Q is used to determine the detonation pressure (PD) and velocity (VD) (Kamlet & Hurwitz, 1968; Keshavarz, 2007). The equations for PD and VD are given in subsection 3.2.2.

2.1.5 Oxygen Balance

The performance of energetic materials depends on the chemical reaction (detonation reaction) of the material (Gilman, 1995; Zhang *et al*., 2009). Detonation occurs when there is no external supply of oxygen contrary to combustion which require supply of oxygen (Gardiner & Burcat, 1984). In this regard, for detonation to occur there must be intra-molecular oxygen sufficient to cause self oxidation of the compound and this is indicated by oxygen balance (OB). The OB is a qualitative indicator of the degree of oxidation of an energetic material (He & Shreeve, 2016; Wu *et al*., 2014). It is a result of sufficient or lack of oxygen atoms in a compound and the OB can be positive, negative or zero. A positive OB indicates that an explosive contains more oxygen than required for complete oxidation (Sun *et al*., 2019). Therefore, all metal atoms will be converted to metal oxides, non-metal to

gaseous non-metal oxides and excess oxygen will remain. For a negative OB it means that the compound contain less oxygen than required and thus more oxygen is required for complete oxidation (He *et al*., 2015). It is always leading to incomplete combustion which is accompanied by release of dangerous gases such as CO (Babkin *et al*., 1991). On the other hand, a zero OB is an indicator that the present oxygen in a compound is just enough to convert metals and non-metals to oxides (Wu *et al*., 2013; Yang *et al*., 2018). That is all carbon atoms to be converted to CO_2, sulfur to SO_2, hydrogen to H_2O and all metals to their respective oxides. Some explosive parameters such as strength, sensitivity and performance depend on OB; as OB approaches zero, these parameters increase dramatically (Licht, 2000; Yan & Zeman, 2013). The OB is expressed as:

$$OB = \frac{1600(z - 2x - m) + 800y}{M_W} \tag{8}$$

where x, y, m and z is the number of carbon, hydrogen, metal and oxygen atoms, respectively, and M_w is the molecular weight of an explosive.

For the compounds involving fluorine while lacking metal atoms, it's convenient to express the OB as α (degree of self-oxidation). The degree of oxidation is based on the number of atoms of all the species present in the compound:

$$\alpha = \frac{2f + g}{4d + e} \tag{9}$$

where d, e, f and g are the number of atoms of carbon, hydrogen, oxygen and fluorine, respectively.

Different values of α have different implication on the sufficiency and insufficiency of oxygen in a molecule necessary for self combustion. That is, if α is greater or equal to one, implies the presence of sufficient number of oxygen in a compound otherwise insufficient oxygen atoms (Dalinger *et al*., 2018).

2.2 Triazoles

A triazole is a diunsaturated heterocyclic organic compound of the formula $C_2H_3N_3$. It has five members in a ring of three nitrogen atoms and two carbon atoms (Kharb *et al*., 2011). Two sets of isomers exist for this compound which differ in the relative positions of the

nitrogen atoms. Each isomer has also two tautomers (Fig. 1) which differ depending on a nitrogen where hydrogen is bonded (Holm & Straub, 2011). They possess donor atoms (nitrogen atoms) in the ring enabling them to have numerous bonding modes including bridging (Holm & Straub, 2011). In 1885, Bladin reported the first triazole formed by reacting formamide and formhydrazine (Pellizzari, 1894; Potts, 1961). Afterwards formamide was condensed with hydrazine sulfate to give highest percentage yield of triazole (50%) which was later improved by treating N, N′- diformylhydrazine with excess NH_3 at 200 ^oC giving up to 80% of triazole (Ainsworth & Jones, 1955; Gibson, 1969; Kovalev & Postovskii, 1971; Lakhan & Ternai, 1974; Petree *et al*., 1981).

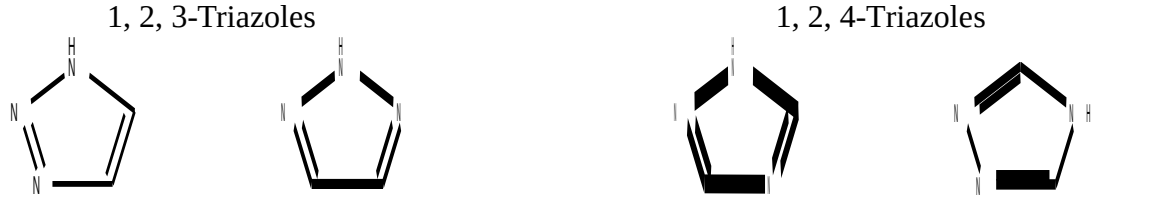

Figure 1: Different triazole structures

High nitrogen heterocycles, for instance triazoles and tetrazoles, provide a good backbones for the development of energetic materials used for various purposes in industries especially mining industry. Such compounds are often chemically modified by various functional groups so that they can acquire a desired set of properties (Zhang *et al*., 2019). A diversity of designs of high energy materials has been based on increasing the number of nitro groups in the heterocycle to enhance their energetic nature (Semenov *et al*., 2017).

2.3 Role of Trinitromethyl Moiety in Energetic Compounds

The requirement for self oxidation of energetic materials has brought the need for the presence of oxygen atoms in the compound (Kettner & Klapötke, 2014; Klapötke, 2019). However, it is desired that the compound detonates faster with lower rate of explosion (Kettner & Klapötke, 2014). Klapötke *et al*. (2014) reported that trinitromethyl moiety is one of the novel oxidizers which does not explode and enables the compound to detonate fast. Generally, the inclusion of nitro group contributes significantly to energetic performance while decreasing the heat of formation (Chavez *et al*., 2013; Chavez *et al*., 2009; Haiges & Christe, 2013).

The modern design of energetic compounds concerns the introduction of explosophore groups (nitro, azido and azo) and energetic moieties such as $C(NO_2)_2F$ and $C(NO_2)_3$ into a nitrogen containing framework so as to increase the density of the compound (Ostrovskii *et al*., 2017; Semenov *et al*., 2017). The $C(NO_2)_3$ moiety is the oxygen-rich group which provides balance for intermolecular combustion leading to nitrogen, water and carbon dioxide release (Sheremetev *et al*., 2012). Therefore, trinitromethyl moieties are responsible for providing oxygen balance of the molecule which facilitates detonation reaction by increasing the pressure and velocity of detonation (Fischer *et al*., 2010; Thottempudi *et al*., 2012).

2.4 Nitrogen Rich Compounds

Nitrogen rich compounds is the best alternative to traditional explosive materials (Gao *et al*., 2020). Additionally, superior oxygen content is the greatest advantage to energetic materials as it improves the performance (Hervé *et al*., 2010). Comparing mono-trinitromethyl triazole, the bistrinitromethyl triazole has higher heat of formation resulted from the increased number of N atoms in the compound (Feng *et al*., 2016; Fischer *et al*., 2012; Ye *et al*., 2005).

Zhang *et al*. (2019) reported a new family of high-energy density materials obtained by combining azo tetrazoles and triazoles resulting to **(1)** 5, 5′-bis(trinitromethyl)-2,2′-azo-tetrazole, **(2)** 5, 5′-bis(trinitromethyl)-1,1′-azo-tetrazole, **(3)** 5, 5′-bis(trinitromethyl)-3,3′-azo-1*H*-1,2,4-triazole, **(4)** 5, 5′-bis(trinitromethyl)-4,4′-azo-1,2,4-triazole, **(5)** 5, 5′-bis(trinitromethyl)-3,3′-azo-1,2,3-triazole, **(6)** 4, 4′-bis(trinitromethyl)-3,3′-azo-1,2,3-triazole as shown in Fig. 2. Among these compounds, 5, 5′-bis(trinitromethyl)-3, 3′-azo-1H-1,2,4-triazole had optimal energetic properties caused by the increase in the number of energetic nitro groups in the compound.

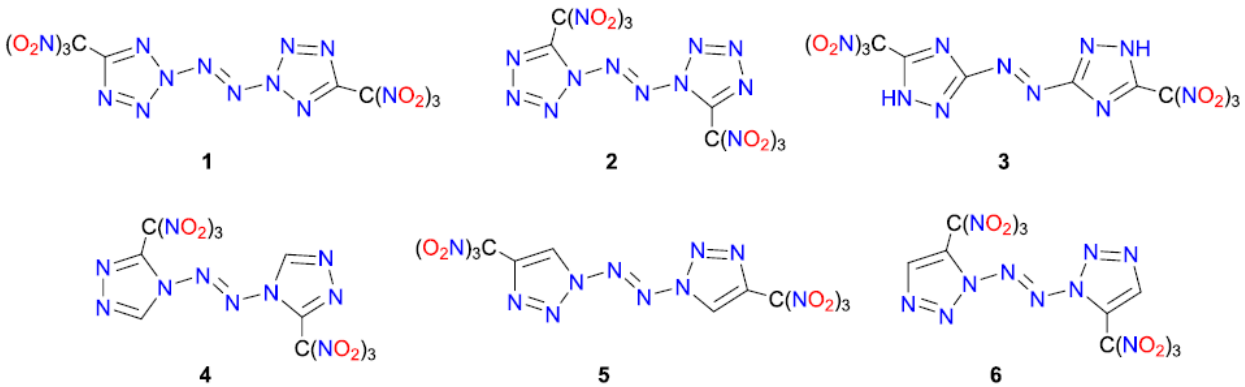

Figure 2: Azo tetrazoles (1, 2) and triazole (3, 4, 5, 6) compounds

The computed energetic properties for the six compounds were compared with known data for common energetic materials (RDX and HMX) and summarized in Table 3 which was retrieved from Zhang *et al*. (2019).

Table 3: Energetic properties of bis(trinitromethyl)-azo-azoles and common energetic materials

Compound	$\Delta_f H°$(c,298) (kJ mol^{-1})	ρ (g cm^{-3})	Q (cal g^{-1})	VD (km s^{-1})	PD (GPa)	OB (%)
1	996.76	1.93	1452	9.11	38.39	13.79
2	1041.75	1.94	1471	9.19	39.15	13.79
3	443.73	1.88	1621	9.10	37.66	3.46
4	1076.08	1.89	1935	9.53	41.37	–3.46
5	732.64	1.87	1759	9.26	38.93	–3.46
6	785.02	1.89	1781	9.34	39.82	–3.46
RDX	79.00	1.80	1501	8.75	34.70	–21.62
HMX	102.41	1.90	1498	9.10	39.30	–21.62

Zhang *et al*. (2019)

Dharavath *et al*. (2017) prepared 5-(dinitromethyl)-3-(trinitromethyl)-1, 2, 4-triazole and its derivatives through the application of oxidative nitration with gem-trinitro compounds. The face-to-face π – π arrangement enforced by an amine fused ring cation caused the advancement of the energetic properties of polynitro azole compounds. They used Fox-7 (1,1-dimino-2,2-dinitroethene) as a precursor, but their synthesis pathway was complex with many procedures. Multifunctional energetic structural materials release energy due to exothermic reactions devised from shock loading conditions. Currently, energetic materials derive their energies from carbon backbones oxidation and possess high enthalpy of formation. Azoles enthalpy of formation varies as the number of catenated nitrogen atoms varies (Liu *et al*., 2019).

Zhang *et al*. (2019), obtained three fluorinated nitrotoluenes (Fig. 3) through nitration processes under elevated temperature. The structures obtained were studied using quantum mechanical calculations and crystalline investigations. Under the developed nitration method, a single nitration product was obtained without isomers.

3,5-difluoro-2,4-dinitrotoluene (DFDNT)

3,5-difluoro-2,4,6-trinitrotoluene (DFTNT)

α,α,α,3,5-pentafluoro-2,4-dinitrotoluene (PFDNT)

Figure 3: DFDNT, DFTNT and PFDNT compounds

Diverse intermolecular interfaces influenced crystal packing; and molecular densities were increased after introducing fluoro groups into trinitrotoluene and dinitrotoluene. But the sensitivities of the prepared compounds were increased relative to that of dinitrotoluene and trinitrotoluene caused by weaker hydrogen bonding interactions (Zhang *et al*., 2019).

Dalinger *et al*. (2018) synthesized novel energetic compounds using N-$C(NO_2)_2NF_2$ and N-$C(NO_2)_2F$ units on the combination of tetrazoles and pyrazole to create energetic biazoles. Among them, the difluoroamine derivative showed the desired energetic properties due to the increased number of fluorine atoms in the molecule. The present study focused on fluorination of triazole derivatives; new high energy density materials were designed via introduction of fluorine atoms into ring/ azo chain of trinitromethyl azo triazoles aimed at enhancing energetic properties.

CHAPTER THREE

MATERIALS AND METHODS

3.1 Compounds Investigated

In this study, new high energy density materials were designed via introduction of fluorine atoms into trinitromethyl azo triazoles aimed at enhancing energetic properties; mono, di, tri and tetra fluorobis(trinitromethyl) azo triazoles molecules (Fig. 4) were proposed and investigated their properties.

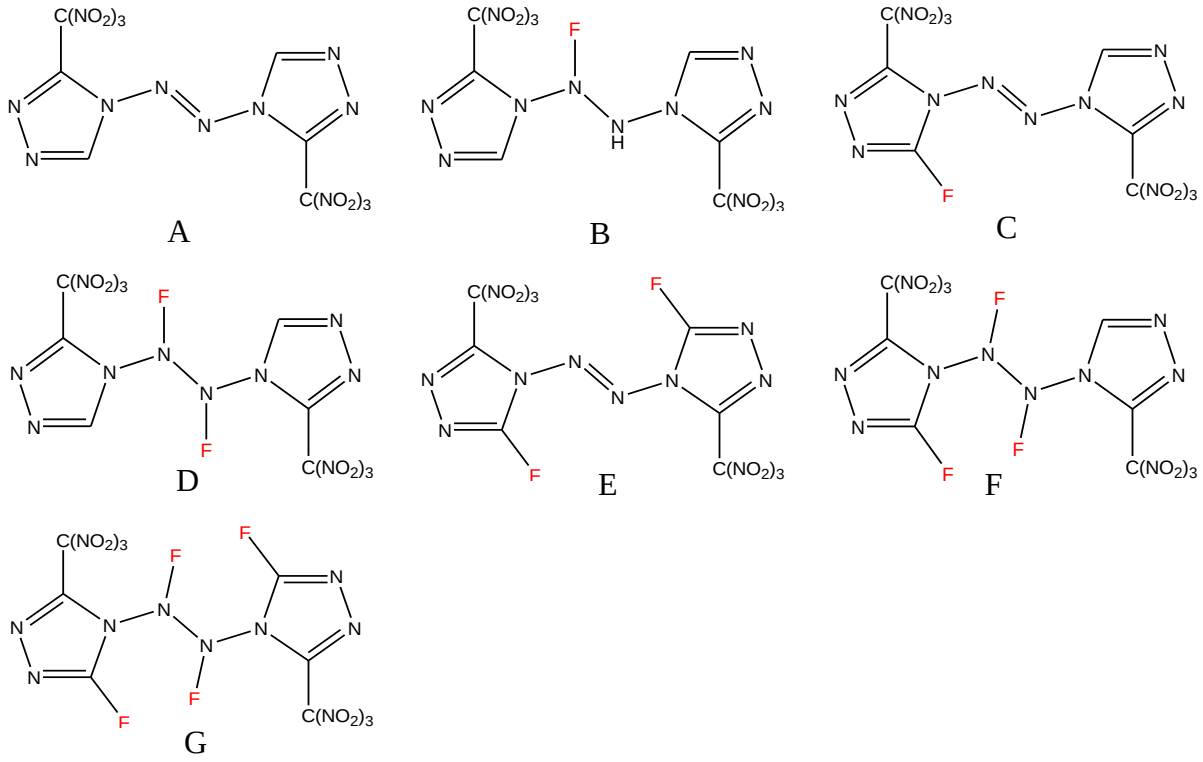

Figure 4: Structural formulae of bis(trinitromethyl) azo triazoles: Non-fluorinated (A) and designed fluorinated molecules (B-G)

3.2 Computational Details

3.2.1 Computations of Structural and Thermodynamic Properties

Density functional theory DFT/B3LYP (Becke, 1993) with 6-31G(d,p) basis set was used for optimization of ground state geometries and frequencies calculations for each molecule. Similar approach was used, for example, by Wei *et al*. (2009) for investigation of tetrazine-based HEDM. The absence of imaginary frequencies confirmed that the obtained geometries corresponded to energy minima on the potential energy surfaces. Quantum chemical calculations were performed with the Gaussian 09 software (Frisch *et al.*, 2009). Thermodynamic characteristics of reactions were obtained with extended 6-311++G(d,p) basis set. Based on the optimized geometrical parameters and vibrational frequencies, the thermodynamic functions (TDF) of gaseous species were calculated applying the 'rigid rotor-harmonic oscillator' approximation with OpenThermo software (Tokarev, 2007). The electrostatic potential surface properties (molecular surface area, volume, charge balance and molecular density) were analyzed using Multiwfn software (Lu & Chen, 2012). Molecular design, visualization of molecular and electronic structures, IR spectra were done by using Avogadro (Ali *et al*., 2012), GaussView05 (Frisch *et al*., 2009) and ChemCraft (Zhurko & Zhurko, 2015) software.

The energies of reactions ($\Delta_r E$) were calculated by considering the difference between the total energies of the products (ΣE_{prod}) and reactants (ΣE_{react}):

$$\Delta_r E = \Sigma E_{prod} - \Sigma E_{react} \quad (10)$$

The enthalpies of the reactions were computed by adding the zero-point vibration energies (Δ_rZPVE) to the $\Delta_r E$:

$$\Delta_r H°(g, 0) = \Delta_r E + \Delta_r \text{ZPVE} \quad (11)$$

To compute the enthalpy of formation of a gaseous species, the enthalpy of formation at 0 K, $\Delta_f H°(g, 0)$ was calculated first, and then enthalpy of formation at 298 K, $\Delta_f H°(g, 298)$:

$$\Delta_f H°(g, 0) = \Sigma \Delta_f H°_{prod}(g, 0) - \Delta_r H°(g, 0) \quad (12)$$

$$\Delta_f H°(g, 298) = \Sigma \Delta_f H°_{prod}(g, 298) - \Delta_r H°(g, 298) \quad (13)$$

$$\Delta_r H°(g, 298) = \Delta_r H°(g, 0) + \Delta_r [H°(g, 298) - H°(g, 0)] \quad (14)$$

where $\Delta_r[H°(g, 298) - H°(g, 0)]$ is the enthalpy increment of the reaction. The enthalpies of formation and enthalpy increments of small gaseous species involved in reaction have been taken from the IVTANTHERMO database (Gurvich *et al*., 1992). For the solid phase species, enthalpies of formation $\Delta_f H°(c, 298)$ were calculated as follows:

$$\Delta_f H°(c, 298) = \Delta_f H°(g, 298) - \Delta_{sub} H°(298) \quad (15)$$

The enthalpy of sublimation $\Delta_{sub} H°(298)$ was obtained as described in (Byrd & Rice, 2006; Karaghiosoff *et al*., 2003; Politzer *et al*., 1997):

$$\Delta_{sub} H°(298) = hA^2 + i(\upsilon\sigma^2_{tot})^{0.5} + j \quad (16)$$

where A is the molecular surface area, $\upsilon\sigma^2_{tot}$ is the electrostatic interaction index; both obtained from the Multiwfn program package (Lu & Chen, 2012); and the h, i, and j are the fitting parameters adopted from Byrd and Rice (2006).

The Gibbs free energy is the measure of reaction spontaneity calculated by the following equation:

$$\Delta_r G°(T) = \Delta_r H°(0) + \Delta_r[H°(T) - H°(0)] - T\Delta_r S°(T) \quad (17)$$

where $\Delta_r[H°(T) - H°(0)]$ is the enthalpy increment and $\Delta_r S°(T)$ entropy of the reaction.

3.2.2 Computations of Energetic Properties

Energetic properties indicate how the materials are powerful upon detonation. They include; molecular density (ρ_{mol}), detonation velocity (VD) and pressure (PD), detonation heat (Q), impact sensitivity ($h_{50\%}$), and oxidation coefficient (α). The density of molecules was estimated in terms of atoms in a molecule (Espinosa *et al*., 1999; Rice *et al*., 1999) as suggested by Politzer (Politzer *et al*., 2009):

$$\rho_{mol} = 0.9183 \left(\frac{M_W}{V}\right) + 0.0028(\upsilon\sigma^2_{tot}) + 0.0443 \quad (18)$$

where V is the volume enclosed by the 0.001 atomic unit contour of electron density of the molecule, M_w is the molar mass of the compound, and $\upsilon\sigma^2_{tot}$ is the index of electrostatic interaction obtained using Multiwfn program package (Lu & Chen, 2012).

The detonation velocity VD and pressure PD indicate how the material is potent upon detonation. The higher are the values of these parameters, the better the performance of the material. The parameters were estimated using the following equations (Fischer *et al*., 2013; Mei *et al*., 2019; Keshavarz, 2005; 2008; Keshavarz & Pouretedal, 2004; Politzer *et al*., 2001; Wang *et al*., 2006):

$$VD = 1.01\left(\sqrt{N\sqrt{MQ}}\right)(1 + 1.30\,\rho_{mol}) \tag{19}$$

$$PD = 1.56\rho^2 N\sqrt{MQ} \tag{20}$$

where N stands for the number of moles of gases produced per gram of the material upon detonation:

$$N = \frac{\Sigma n_{prod}}{M_W} \tag{21}$$

Hence the inverse N gives the average molecular mass M of all detonation products:

$$M = \frac{M_W}{\Sigma n_{prod}} \tag{22}$$

The detonation heat is:

$$Q = -\left(\frac{\sum \Delta_f H^{o}{}_{prod}(g,\ 298) - \Delta_f H^{o}(c,298)}{M_W}\right) \tag{23}$$

The impact sensitivity, $h_{50\%}$ was obtained using the generalized interact property function (Mei *et al*., 2019; Rice & Hare, 2002):

$$h_{50\%} = 29.3 + 0.001386\exp(48.84\upsilon) \tag{24}$$

where υ is the index of charge balance obtained using Multiwfn program package (Lu & Chen, 2012).

The coefficient of oxidation α indicates how well the material provides its own oxidant (Dalinger *et al*., 2018). The increase in α increases the ability of the materials' self-oxidation

(Dalinger *et al*., 2018). For the compound with the molecular formula $C_xH_yN_wO_zF_v$, the coefficient of oxidation is estimated as follows (Dalinger *et al*., 2018):

$$\alpha = \frac{\left(z + \frac{v}{2}\right)}{\left(2x + \frac{y}{2}\right)} \tag{25}$$

The computational details are summarized in Table 4.

Table 4: Summary of computational details

Procedures/Properties	Software/Method	Refs
(i) Molecular design (ii) Drawing the structure of molecules (iii) Visualization of inputs and outputs	Avogadro	Ali *et al*. (2012)
(iv) Optimization of geometric structures (v) Vibration spectra	Gaussian 09, DFT/ B3LYP/6-31G(d,p)	Frisch *et al*. (2009)
(vi) Electrostatic potential surface analysis (molecular surface area, volume, charge balance, variation, and molecular density)	Multiwfn	Lu and Chen (2012)
Thermodynamics of decomposition and combustion reactions:	Gaussian 09, DFT/ B3LYP/6-311++G(d,p)	
(vii) TDF of the designed species	OpenThermo;	Tokarev (2007)
(viii) Reference data (TDF and enthalpies of formation) of the reactions products	IVTANTHERMO Database	Gurvich *et al*. (1992)
(ix) Visualization of molecular structures, IR spectra	GaussView05; ChemCraft	Frisch *et al*. (2009) Zhurko and Zhurko (2015)

CHAPTER FOUR

RESULTS AND DISCUSSION

4.1 Geometrical Properties of Fluorinated Triazole Derivatives

The design started from the trinitromethyl azo triazole and then introduced fluorine atoms into azo group or/and triazole rings replacing the available hydrogen atoms. It is anticipated that introduction of fluorine atoms and the presence of trinitromethyl moieties will contribute to the energy density while azo and triazole skeleton rings will increase the stability of the molecule.

The optimized configurations of the molecules are shown in Fig. 5; the most relevant geometrical parameters are given in Table 5.

Table 5: Selected optimized geometrical parameters of non-fluorinated (A) and designed fluorinated bridged triazole derivatives (B-G)

Molecule	$R_{1,2,3}$(N-N)	$R_{1,2}$(N-F)	$R_{1,2}$(C-F)	$\alpha_{1,2}$(N-C-N)	χ(N-N-N-N)	$\phi_{1,2}$(C-N-N-C)
A	1.368, 1.246, 1.368			110.0, 110.0	180.0	180.0, 180.0
B	1.390, 1.464, 1.295	1.420		110.0, 110.0	176.0	176.0, 179.0
C	1.371, 1.246, 1.365		1.304	112.0, 110.0	179.0	175.0, 176.0
D	1.377, 1.506, 1.376	1.414, 1.414		109.0, 109.0	174.0	173.0, 175.0
E	1.370, 1.246, 1.370		1.304, 1.304	112.0, 112.0	180.0	180.0, 180.0
F	1.376, 1.511, 1.376	1.414, 1.414	1.303	112.0, 110.0	173.0	175.0, 173.0
G	1.380, 1.423, 1.379	1.417, 1.420	1.302	112.0, 112.0	154.0	78.0, 172.0

Note: Bond lengths (Å), bond angles (°) and dihedral angles (°)

$R_{1,2,3}$(N-N) are $R_1(N_3\text{-}N_4)$, $R_2(N_4\text{-}N_5)$ and $R_3(N_5\text{-}N_6)$

$R_{1,2}$(C-F) are left and right side, equivalent bonds

$R_{1,2}$(N-F) are the bond lengths on the azo group $R_1(N_4\text{-}F)$, $R_2(N_5\text{-}F)$

$\alpha_{1,2}$(N-C-N) are the bond angles $\alpha_1(N_2\text{-}C_2\text{-}N_3)$ and $\alpha_2(N_6\text{-}C_3\text{-}N_7)$ in the left and right triazole rings, respectively.

$\varphi_{1,2}$(C-N-N-C) are the dihedral angles $\varphi_1(C_1\text{-}N_3\text{-}N_6\text{-}C_4)$ and $\varphi_2(C_2\text{-}N_4\text{-}N_5\text{-}C_3)$ between two azo rings.

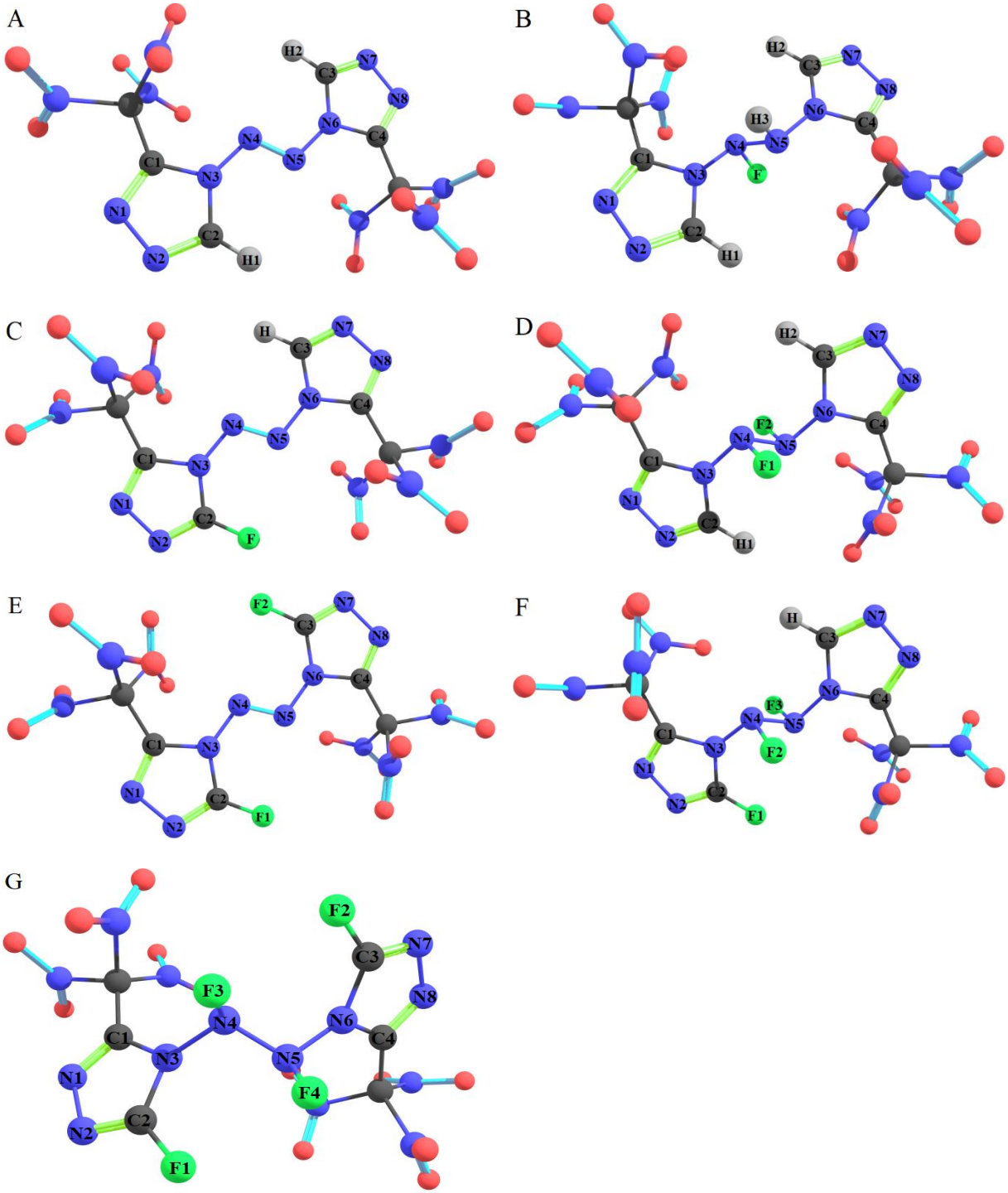

Figure 5: Optimized molecular structures of non-fluorinated (A) and designed fluorinated bridged triazole derivatives (B-G)

The analysis of the optimized parameters shows that the addition of fluorine atoms to the original trinitromethyl azo triazole molecule A affects mostly the nearest bonds as well as the planarity of the structure. In the molecules B, D, F and G where the F-atoms are added to the azo chain, the formed N-F bonds are maintained perpendicular to the chain moiety and the central double N=N bond transforms into the single bond which brings an elongation of the

$R_2(N_4\text{-}N_5)$ from 1.246 up to 1.511 Å. When the fluorine atoms are attached to the triazole rings (molecules C, E, F, G), they just replace the hydrogen atoms forming alike C-F bonds of 1.302 – 1.304 Å length while keeping the rings coplanarity and slightly increasing bond angles N-C-N from 109° to 112°. All compounds except G have close to a coplanar structure, dihedral angles between the rings and in the chain N-N-N-N range from 173° to 180°, whereas the molecule G with four F atoms, two at the chain and two at the rings, has a bent configuration with the angles $\varphi_1(C_1\text{-}N_3\text{-}N_6\text{-}C_4) = 78°$ and $\chi(\text{N-N-N-N}) = 154°$.

4.2 Vibrational Analysis

The computed vibrational spectra of the designed molecules confirmed the absence of imaginary frequencies; the simulated IR absorption spectra are shown in Fig. 6. For all compounds, most intensive peaks between ~1700 and 1740 cm^{-1} are assigned to asymmetric stretching of N=O bonds in the trinitromethyl moieties and lower peaks between 806 and 815 cm^{-1} to bending vibrations of the same bonds. Other strong absorptions near 1350 cm^{-1} and 1370-1430 cm^{-1} correspond to stretching vibrations of C-N bonds of the trinitromethyl moieties and C-N bonds of the triazole rings, respectively. Besides, there are weak absorption peaks at ~600-740 cm^{-1} which correspond to the bending vibrations of the triazole rings. For the fluorinated compounds B, D, F and G, the stretching vibrations of N-F bonds of the hydrazine group are seen at ~900-955 cm^{-1}. For the molecules C, E, F and G, the sharp absorption peaks at ~1650 cm^{-1} correspond to C-F stretching of the triazole skeleton.

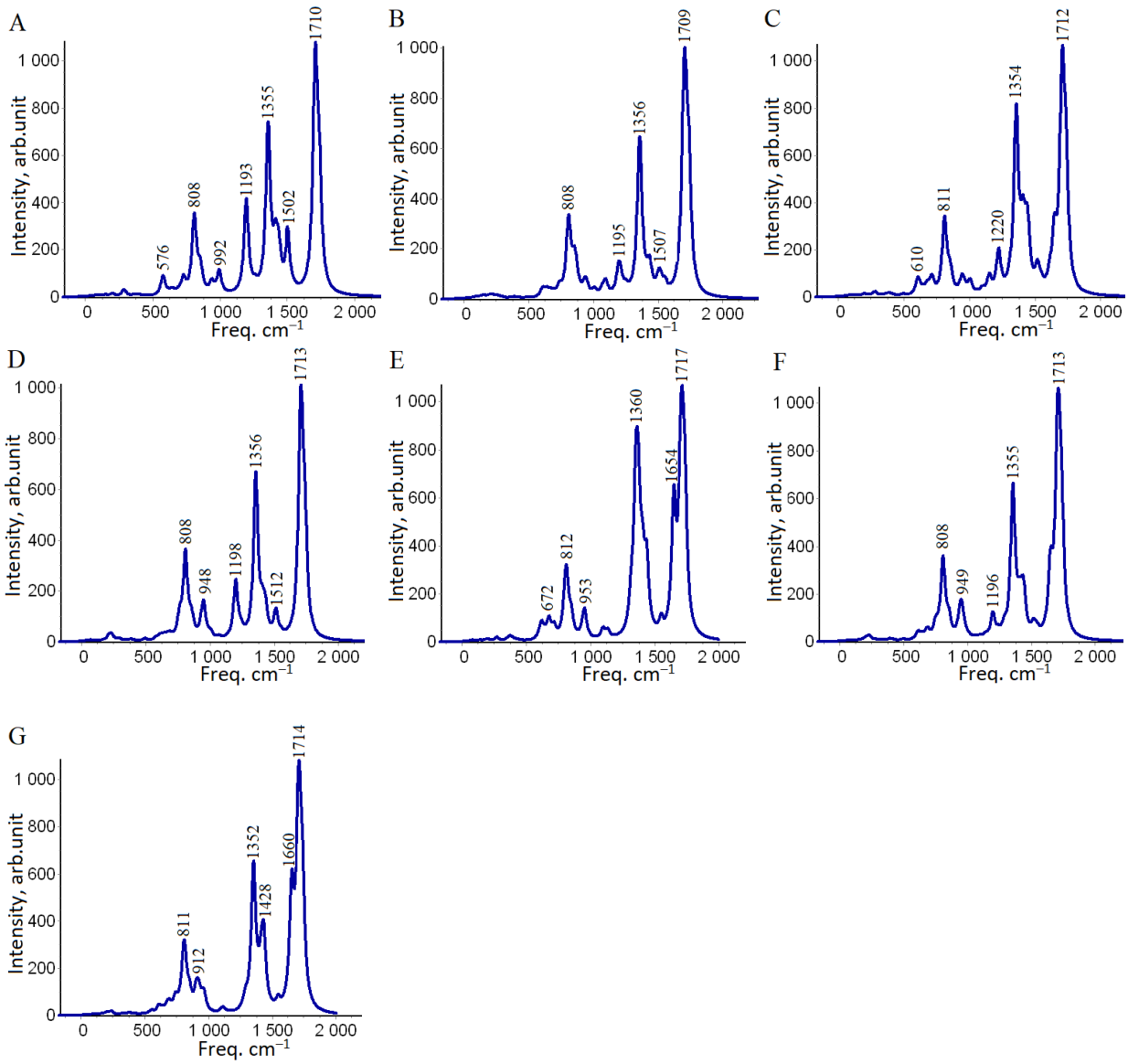

Figure 6: Computed infrared spectra of non-fluorinated (A) and fluorinated (B-G) bridged triazole derivatives

4.3 Electronic Structure of Gaseous Molecules

The intramolecular charge transfer within the material can be understood through molecular orbitals analysis. It is expected that good HEDM should have a distinct separation of electron density between the HOMO and LUMO and reasonably small energy gap E_g for electrons transition. Also, it was noticed that in some cases a correlation between energy gap and sensitivity of the explosive materials may exist (Gu *et al*., 2014; Michalchuk *et al*., 2019). Negative correlation between energy gap and detonation velocity or pressure was reported in (Mukhanov, 2014). For the seven compounds A-G, the frontier molecular orbitals and energy

gaps are displayed in Fig. 7. The green colour denotes the negative phase, and deep red indicates the positive phase.

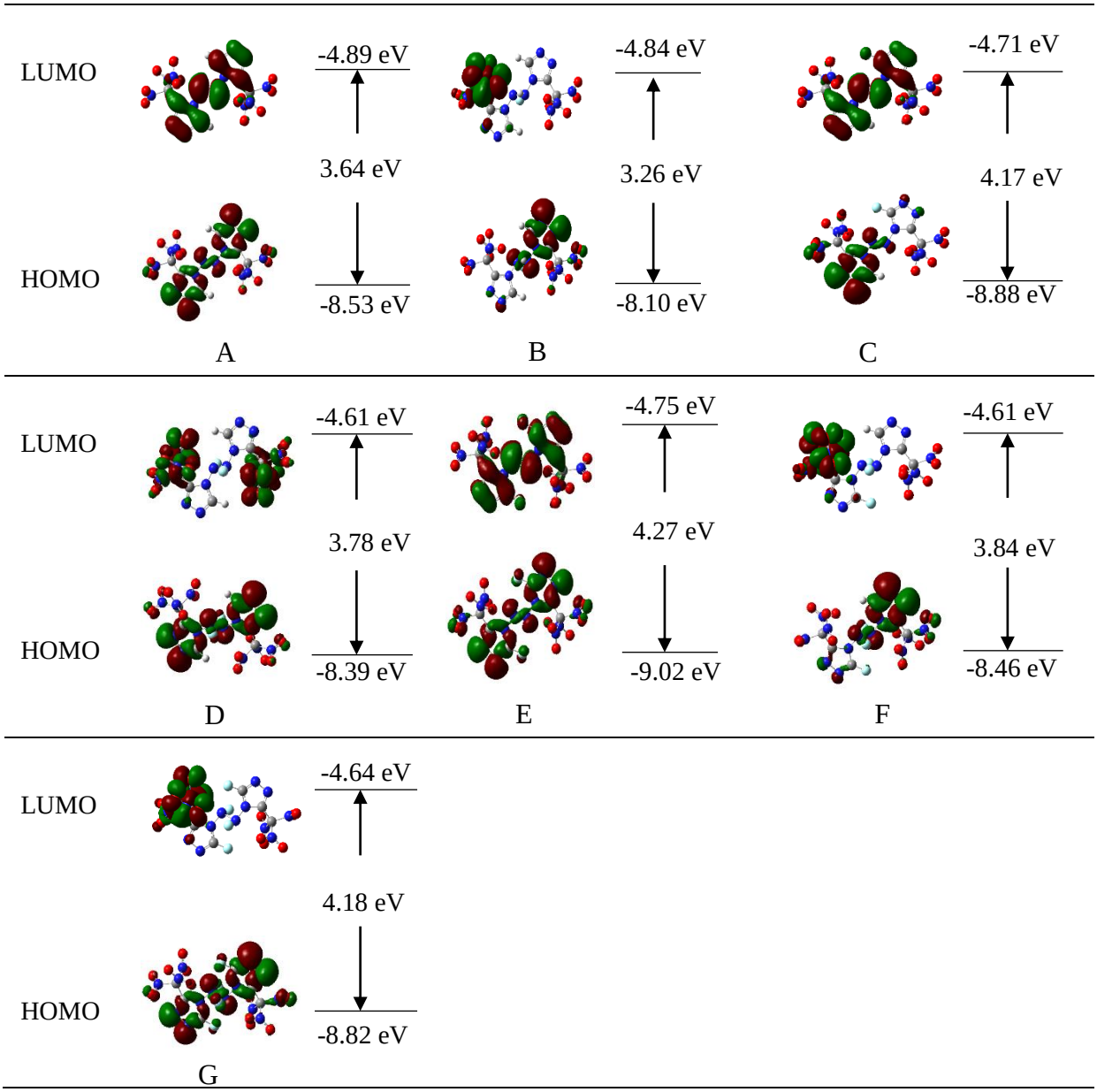

Figure 7: Graphical representation of HOMO and LUMO isosurfaces, energy gaps, and energies of molecules A–G

Higher electron density is found near atoms/groups which possess higher electronegativity; here they are fluorine and nitrogen atoms in the rings or nitro groups. Redistribution of electron density between the HOMO and LUMO is clearly seen for the fluorinated species B, D, F and G while not observed for others (A, C and E). Therefore, the fluorine attachment to the hydrazine chain favours the transfer of electrons in the HOMO→LUMO transition. The energy gap increases upon fluorine attachment to the triazole rings, A (3.64 eV) < C (4.17 eV) < E (4.27 eV), but when F atoms join the central hydrazine group, the E_g decreases, B

(3.26 eV) < D (3.78 eV) < F (3.84 eV) < G (4.18 eV). The highest E_g = 4.27 eV is obtained for the E compound and the lowest E_g = 3.26 eV is for B molecule. This indicates that the addition of fluorine on the azo chain is helpful in decreasing the energy gap. These values are comparable to the experimental E_g values for traditional explosive compounds; 3.4 eV (RDX) (Perger, 2003), 4.27 eV (PETN) (Mukhanov, 2014) and 5.32 eV (HMX) (Mukhanov, 2014). Therefore, the compounds B and D for which the requirements of good electron density separation and smaller energy gaps are met, are anticipated to be better HEDM.

4.4 Thermodynamics of Detonation and Combustion Gaseous Reactions

Detonation and combustion reactions with formation of simple products CO, CO_2, H_2O, HF, F_2 and others, have been considered for gaseous compounds A-G (Table 2). Energies $\Delta_r E$ and enthalpies $\Delta_r H°(0)$ of the reactions have been computed using equations (11) and (12). As is seen, all reactions considered are highly exothermic; the values of $\Delta_r H°(0)$ vary from −374 to −4499 kJ mol^{-1}. Generally, the biggest amount of energy released through detonation channels with the formation of CO_2, N_2, HF/F_2 and the smallest enthalpy of detonation is observed for the reactions A4-G4 with the C, CO and O_2 products. Clearly seen that fluorination of the bridged trinitromethyl azo triazole alters the heat effect. That is in accordance with findings by other researchers (Dalinger *et al*., 2018; Martinez *et al*., 2012; Ye *et al*., 2007; Zhang *et al*., 2019) that most exothermic reactions relate to the hydrogen fluoride being formed among the products. If compare the enthalpies of most exothermic detonation reactions, i.e. A1-G1, the values of $\Delta_r H°(0)$ become more negative due to the azo-chain fluorination in the absence of triazole ring fluorination, from −3367 (A1) up to −4216 (B1) and −3923 kJ mol^{-1} (D1); whereas fluorination of the rings brings to lower heat effect in reactions C1, E1-G1 than for the non-fluorinated original compound (A1).

Table 6: Thermodynamic characteristics of gas phase reactions and enthalpies of formation of gaseous compounds, all values in kJ mol^{-1}

	Equation of chemical reaction	$-\Delta_r E$	$-\Delta_r$ZPVE	$-\Delta_r H°(0)$	$\Delta_r[H°(298) - H°(0)]$	$\Delta_f H°(0)$	$\Delta_f H°(298)$
A1	$C_6H_2N_{14}O_{12} = CO + 5CO_2 + 7N_2 + H_2O$	3237.7	129.0	3366.6	47.11	1048.2	1095.3
A2	$C_6H_2N_{14}O_{12} = 0.5C + 5.5CO_2 + 7N_2 + H_2O$	2897.3	126.9	3024.2	46.01	978.5	1024.5
A3	$C_6H_2N_{14}O_{12} = 6CO + 7N_2 + H_2O + 2.5O_2$	1758.8	191.8	1950.6	69.17	1028.8	1098.0
A4	$C_6H_2N_{14}O_{12} = 5CO + C + 7N_2 + H_2O + 3O_2$	782.3	200.2	982.4	71.38	885.7	957.0
A5	$C_6H_2N_{14}O_{12} + 0.5O_2 = 6CO_2 + 7N_2 + H_2O$	3533.4	116.4	3649.8	42.70	1052.0	1094.7
	Average $\Delta_f H°$(A, g)					999±70	1054±62
B1	$C_6H_3N_{14}O_{12}F = CO + 5CO_2 + 7N_2 + H_2O + HF$	4072.5	143.6	4216.1	52.3	994.3	1046.6
B2	$C_6H_3N_{14}O_{12}F = 0.5C + 5.5CO_2 + 7N_2 + H_2O + HF$	3732.1	141.5	3873.6	55.4	924.6	980.0
B3	$C_6H_3N_{14}O_{12}F = 6CO + 7N_2 + H_2O + 2.5O_2 + HF$	2593.6	206.5	2800.0	74.4	974.9	1049.3
B4	$C_6H_3N_{14}O_{12}F = 5CO + C + 7N_2 + H_2O + 3O_2 + HF$	1617.1	214.8	1831.9	76.6	831.8	908.3
B5	$C_6H_3N_{14}O_{12}F + 0.5O_2 = 6CO_2 + 7N_2 + H_2O + HF$	4368.2	131.0	4499.3	52.5	998.1	1050.6
	Average $\Delta_f H°$(B, g)					945±70	1007±63
C1	$C_6H_1N_{14}O_{12}F = 6CO_2 + 7N_2 + HF$	3414.0	121.8	3535.8	43.4	903.6	947.0
C2	$C_6H_1N_{14}O_{12}F = 0.5CO + 5.5CO_2 + 7N_2 + 0.5H_2O + 0.5F_2$	3109.0	124.1	3233.1	48.4	894.4	942.8
C3	$C_6H_1N_{14}O_{12}F = 6CO + 7N_2 + 3O_2 + HF$	1639.3	197.2	1836.5	69.9	880.4	950.3
C4	$C_6H_1N_{14}O_{12}F = 5CO + C + 7N_2 + 0.5H_2O + 3.25O_2 + 0.5F_2$	505.7	201.6	707.3	70.7	730.0	800.7
C5	$C_6H_1N_{14}O_{12}F + 0.25O_2 = 6CO_2 + 7N_2 + 0.5H_2O + 0.5F_2$	3256.9	117.8	3374.7	42.0	896.4	933.9
	Average $\Delta_f H°$(C, g)					861±74	915±64
D1	$C_6H_2N_{14}O_{12}F_2 = 6CO_2 + 7N_2 + 2HF$	3791.9	130.6	3922.6	48.4	1017.2	1065.6
D2	$C_6H_2N_{14}O_{12}F_2 = 0.5C + 5.5CO_2 + 7N_2 + H_2O + F_2$	2841.5	133.2	2974.8	53.1	929.1	982.3
D3	$C_6H_2N_{14}O_{12}F_2 = 6CO + 7N_2 + 3O_2 + HF$	2017.2	206.1	2223.3	74.9	994.0	1068.8

	Equation of chemical reaction	$-\Delta_r E$	$-\Delta_r$ZPVE	$-\Delta_r H°(0)$	$\Delta_r[H°(298) - H°(0)]$	$\Delta_f H°(0)$	$\Delta_f H°(298)$
D4	$C_6H_2N_{14}O_{12}F_2 = 5CO + C + 7N_2 + 3.5O_2 + 2HF$	1040.7	214.4	1255.2	77.1	850.8	927.9
D5	$C_6H_2N_{14}O_{12}F_2 + 0.5O_2 = 6CO_2 + 7N_2 + H_2O + F_2$	3477.7	122.8	3600.5	50.2	1002.7	1052.9
	Average $\Delta_f H°$(D, g)					959±69	1020±62
E1	$C_6N_{14}O_{12}F_2 = 6CO_2 + 7N_2 + F_2$	2980.0	119.2	3099.2	45.8	740.4	786.2
E2	$C_6N_{14}O_{12}F_2 = 0.5C + 5.5CO_2 + 7N_2 + 0.5O_2 + F_2$	2343.9	129.6	2473.6	48.7	666.8	715.6
E3	$C_6N_{14}O_{12}F_2 = 6CO + 7N_2 + 3O_2 + F_2$	1205.4	194.6	1400.0	67.7	717.1	784.8
E4	$C_6N_{14}O_{12}F_2 = 5CO + C + 7N_2 + 3.5O_2 + F_2$	228.9	203.0	431.8	69.9	574.0	643.9
E5	$C_6N_{14}O_{12}F_2 + 0.5O_2 = 6CO_2 + 7N_2 + F_2O$	2953.3	116.1	3069.3	43.6	737.2	780.8
	Average $\Delta_f H°$(E, g)					687±70	742±63
F1	$C_6H_1N_{14}O_{12}F_3 = 6CO_2 + 7N_2 + HF + F_2$	3345.5	128.6	3474.1	46.4	841.9	888.3
F2	$C_6H_1N_{14}O_{12}F_3 = 0.5CO + 5.5CO_2 + 7N_2 + 0.5H_2O + 1.5F_2$	3040.5	131.0	3171.4	47.2	832.8	794.1
F3	$C_6H_1N_{14}O_{12}F_3 = 6CO + 7N_2 + 3O_2 + HF + F_2$	1570.8	204.0	1774.8	72.8	818.7	891.6
F4	$C_6H_1N_{14}O_{12}F_3 = 5CO + C + 7N_2 + 0.5H_2O + 3.25O_2 + 1.5F_2$	437.2	208.4	645.6	73.6	668.3	742.0
F5	$C_6H_1N_{14}O_{12}F_3 + 0.25O_2 = 6CO_2 + 7N_2 + 0.5\ H_2O + 1.5F_2$	3188.4	124.7	3313.0	45.0	834.7	769.9
	Average $\Delta_f H°$(F, g)					799±74	817±69
G1	$C_6N_{14}O_{12}F_4 = 6CO_2 + 7N_2 + 2F_2$	2915.7	126.0	3041.8	48.9	682.9	731.8
G2	$C_6N_{14}O_{12}F_4 = 0.5C + 5.5CO_2 + 7N_2 + 0.5O_2 + 2F_2$	2279.6	136.5	2416.1	51.9	609.4	661.3
G3	$C_6N_{14}O_{12}F_4 = 6CO + 7N_2 + 3O_2 + 2F_2$	1141.1	201.5	1342.5	70.8	659.7	730.5
G4	$C_6N_{14}O_{12}F_4 = 5CO + C + 7N_2 + 3.5O_2 + 2F_2$	164.6	209.8	374.4	73.0	516.5	589.5
G5	$C_6N_{14}O_{12}F_4 + O_2 = 6CO_2 + 7N_2 + 2F_2O$	2862.2	119.8	2982.0	44.4	676.6	721.1
	Average $\Delta_f H°$(G, g)					629±69	687±62

The enthalpies of most exothermic detonation reactions (A1-G1) and combustion reactions (A5-G5) are shown in Fig. 8.

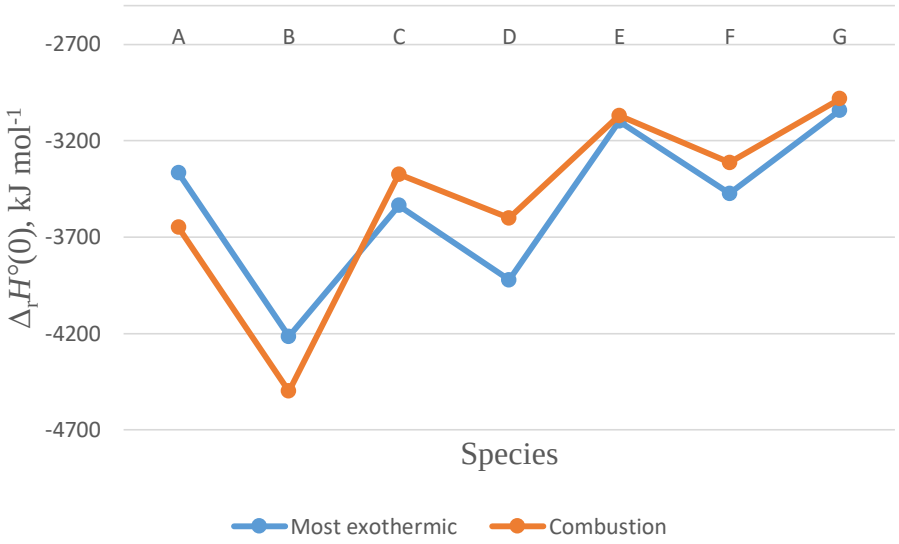

Figure 8: Enthalpies of gaseous detonation and combustion reactions against molecular species

A symbatic behaviour is well seen for the enthalpies of detonation and combustion reactions with maxima for E and G and minima for B and D. Worth to note, for the A and B molecules, combustion is more exothermic compared to detonation. For both types of reactions, the $\Delta_r H°(0)$ becomes more negative as the fluorine atoms are attached on the hydrazine chain and less negative under ring fluorination. Among all compounds, the molecules B and D with one and two F atoms attached to the azo-chain have most negative enthalpies of the reactions.

The computed enthalpies of the reactions $\Delta_r H°(0)$ and enthalpy increments $\Delta_r[H°(298) - H°(0)]$ have been used to obtain enthalpies of formation $\Delta_f H°(0)$ and $\Delta_f H°(298)$ of the gaseous species according to equations (12, 13) and (14). The averaged values of enthalpies of formations over all five reactions have been calculated for each compound, the uncertainties are estimated as standard deviations (Table 6). The thermodynamic properties of individual gaseous species A-G, enthalpies of formation $\Delta_f H°(298)$ and entropies $S°(298)$, are displayed in Fig. 9.

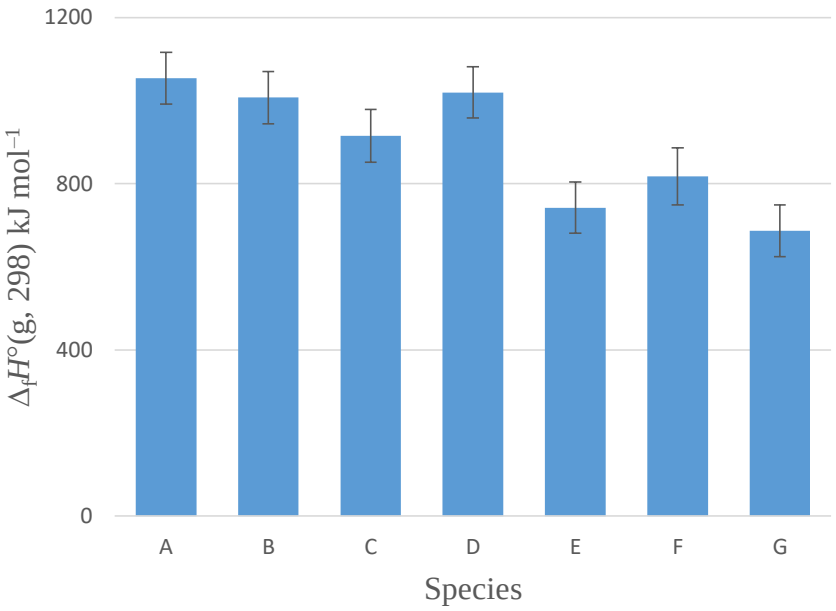

(a)

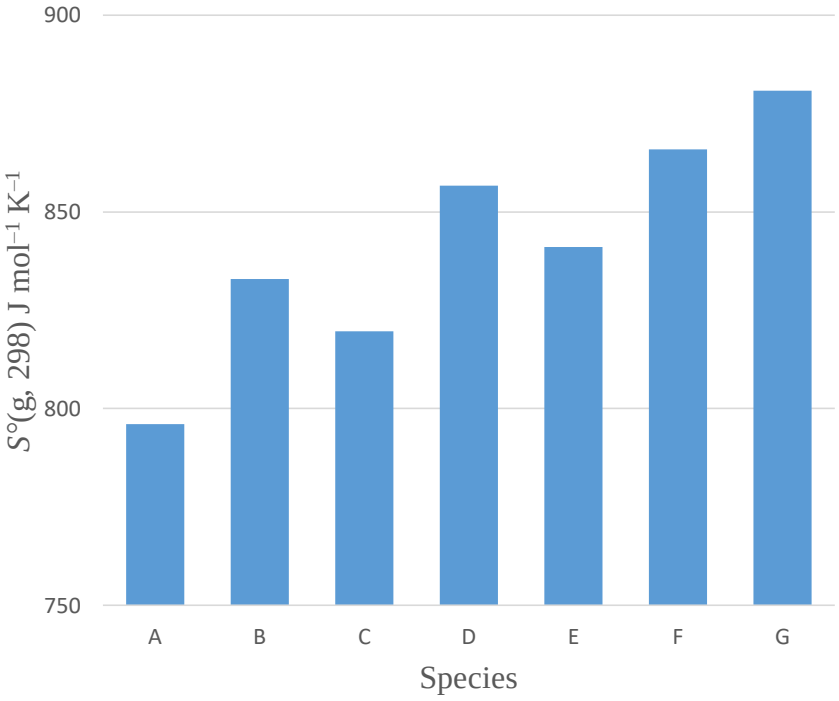

(b)

Figure 9: Thermodynamic characteristics of gaseous species A-G: (a) enthalpies of formation $\Delta_f H°$(g, 298); (b) entropies $S°$(g, 298)

It is observed generally that the consequent addition of fluorine atoms to the molecule from A to G results in irregular change of both characteristics. The position of the F atoms influences the alteration; the hydrazine chain fluorination brings to a larger change of both $\Delta_f H°$(g, 298) and $S°$(g, 298) compared to the triazole rings fluorination. The most distorted geometry of the

G compound which contains four F atoms, two on the hydrazine chain and two on the rings, evidently promotes the greatest entropy among all species.

Temperature dependences of the TDF for different decomposition reactions were also considered. For most exothermic detonation reactions A1-G1, the entropies $\Delta_r S°(T)$ and Gibbs free energies $\Delta_r G°(T)$ over a broad temperature range are presented in Fig. 10. The entropies of all reactions are positive and rather high (Fig. 10a); at room temperature the values of $\Delta_r S°(298)$ range from ~1980 (D1) to 2150 J mol^{-1} K^{-1} (F1 and G1); which is apparently attributed to the greater number of detonation products, 15 moles of products formed from one mole of reactant. There are two groups of curves distinguished; the first one of lower $\Delta_r S°(T)$ combines three decay reactions, of the original (A1) and triazole rings fluorinated compounds (C1, E1). The second one of higher $\Delta_r S°(T)$ combines the reactions of the rest four species, each of them having F atoms at the hydrazine chain. In both groups, the entropies $\Delta_r S°(T)$ slightly decrease by ~ 100 J mol^{-1} K^{-1} subject to temperature increase to 1000 K.

The temperature dependences of Gibbs energies of the reactions have been computed using equation (10), and the results are presented in Fig. 10b. The values of $\Delta_r G°(T)$ are negative attributing to exothermicity of the reactions and positive $\Delta_r S°(T)$, and keep on descending with temperature rise depending on the number and position of attachment of fluorine atoms. Therefore, all reactions are predicted to be spontaneous; moreover, only hydrazine chain fluorinated compounds (B and D) show higher numerical values of Gibbs energy compared to the ring fluorinated (C, E, F and G) and non-fluorinated (A) species.

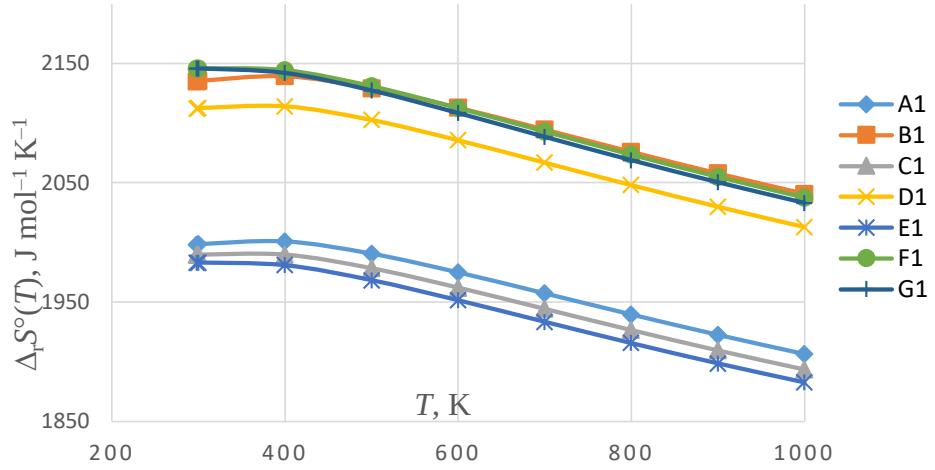

(a)

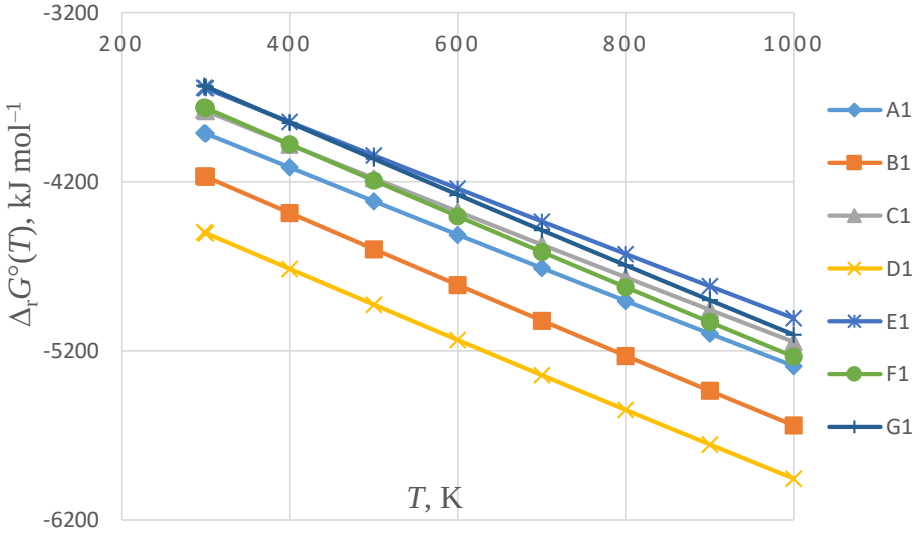

(b)

Figure 10: Temperature dependences of (a) entropies $\Delta_r S°(T)$ and (b) Gibbs free energies $\Delta_r G°(T)$ of most exothermic detonation reactions

4.5 Energetic Properties of Solid Energetic Compounds

Energetic properties include several characteristics of the materials which signify strength, stability and ability to detonate. These properties, enthalpies of formation of solid compounds $\Delta_f H°$(c, 298), molecular density ρ_{mol}, the heat of detonation Q, detonation velocity VD and pressure PD, impact sensitivity $h_{50\%}$, and coefficient of oxidation α, calculated by using equations (18) – (25) for seven compounds A-G, are presented in Table 7; for comparison, two conventional explosives (RDX and HMX) and four nearly related energetic compounds

reported earlier in literature (Byrd & Rice, 2006; Mei *et al*., 2019; Zhang *et al*., 2019; Jin *et al*., 2014; Politzer & Murray, 2011; Rice *et al*., 1999) are also considered.

Table 7: The energetic properties of the compounds A-G, together with related energetic compounds reported in literature

Compound	$\Delta_f H°$(c, 298) kJ mol^{-1}	ρ_{mol} g cm^{-3}	Q cal g^{-1}	VD km s^{-1}	PD GPa	$h_{50\%}$ cm	α
A, $C_6H_2N_{14}O_{12}$	862 ± 62	1.96	1646	9.5	42.3	30.8	0.92
B, $C_6H_3N_{14}O_{12}F$	811 ± 63	1.98	1688	9.7	44.3	32.0	0.93
C, $C_6H_1N_{14}O_{12}F$	724 ± 64	2.01	1672	9.6	44.0	30.1	1.00
D, $C_6H_2N_{14}O_{12}F_2$	868 ± 62	2.03	1691	9.8	45.5	33.1	1.00
E, $C_6N_{14}O_{12}F_2$	551 ± 63	2.07	1398	9.3	41.6	29.8	1.08
F, $C_6H_1N_{14}O_{12}F_3$	623 ± 69	2.09	1367	9.4	42.6	31.1	1.08
G, $C_6N_{14}O_{12}F_4$	492 ± 62	2.14	1272	9.3	42.4	30.1	1.17
RDX[a]	79.0	1.80	1501	8.8	34.7	28.0	0.67
HMX[b]	102.4	1.90	1498	9.1	39.3	32.0	0.67
$C_4H_6N_8O_4$[c]	592.1	1.82	1574	8.7	33.4		
$C_6H_2N_{14}O_{12}$[d]	443.7	1.88	1621	9.1	37.7		
$C_3H_2N_{12}O_5$[e]	740.6	1.82	1605	8.9	35.7		
$C_6H_6N_{12}O_{12}$[f]		2.04	1567	9.4	44.1		

[a] Byrd and Rice (2006), Mei *et al*. (2019), Zhang *et al*. (2019)
[b] Mei *et al*. (2019), Zhang *et al*. (2019), Rice *et al*. (1999)
[c] Jin *et al*. (2014)
[d] Zhang *et al*. (2019)
[e] Mei *et al*. (2019)
[f] Politzer and Murray (2011)

The enthalpies of sublimation $\Delta_{sub}H°(298)$ of the compounds A-G have been evaluated using equation (15) and found to be close from one molecule to another within the range from 192 to 196 kJ mol^{-1}. Based on the $\Delta_{sub}H°(298)$ and enthalpies of formation of gaseous species $\Delta_f H°$(g, 298), the enthalpies of formation of solid compounds A-G $\Delta_f H°$(c, 298) have been obtained by equation (15). For all solid compounds A-G, the enthalpies $\Delta_f H°$(c, 298) are positive, from ~500 to 900 kJ mol^{-1} and change depending on the position attachment of fluorine atoms (the trend is similar to that for gaseous species in Fig. 9a). The calculated enthalpies of formation for the compounds A-G are compared to nearly related explosives reported earlier in Table 7. Due to fluorination, the enthalpies of formation of all designed

compounds are much higher than those of common explosives, 79.0 kJ mol^{-1} (RDX) and 102.4 kJ mol^{-1} (HMX).

Density is one of the significant properties the material must possess as it accounts for its strength; the higher the density, the stronger the material and hence more energy the material will produce upon detonation. It is observed that for all compounds considered in this study the density increases as the number of fluorine atoms is increased. The range of densities is from 1.96 g cm^{-3} for the non-fluorinated molecule A to 2.14 g cm^{-3} for a highly fluorinated G. The increase in densities can be justified by high mass of fluorine atom with small effect on the volume of the molecule and strong π–bonding between the triazole rings and azo/hydrazine group resulting into dense packing. The values of ρ_{mol} for the A-G species are comparable to those for nearly related materials reported in the literature, which are in the range 1.80 – 2.04 g cm^{-3} (Table 7).

Detonation heat is a measure of the material strength and stability as it signifies the amount of energy released as the material detonates. The performance of the material is estimated depending on the value of Q; the higher the value of Q, the greater the material's performance. The detonation heats have been computed using equation (23) for most exothermic detonation processes A1-G1 where the enthalpies of formation of solid reactants $\Delta_f H°$(c, 298) have been taken into account. Among all designed compounds, B, C and D have higher detonation heat Q greater than 1600 cal g^{-1}. This may be due to hydrazine chain fluorination as well as sufficient number of hydrogen atoms in a molecule for complete detonation. Still, these Q values are close to those of reference and original compounds. Worth to note that fluorination of the triazole rings does not bring the elevation of the detonation heat.

The detonation velocity VD and pressure PD are the indicators of HEDM performance. It is expected for the best material to have high detonation velocity and pressure. As seen from Table 7, the designed compounds B, C and D show a slight elevation in VD from 9.5 km s^{-1} for the original A to 9.8 km s^{-1} for D that is a bit greater compared to the reference materials, 8.7 – 9.4 km s^{-1}. There is a rise in pressures of detonation from ~42 GPa for non-fluorinated compound A to ~46 GPa for di-fluorinated compound D. This can be associated with the number of hydrazine fluorinated bonds in these molecules. Among all, the B and D have the highest pressures. The values of PD are comparable to those of nearly related and traditional energetic materials HMX (39.3 GPa) and $C_6H_6N_{12}O_{12}$ (44.1 GPa). The elevation in

detonation pressures and velocity observed for some of the designed species is an indication that fluorination helps in increasing the energy density of the materials.

The impact sensitivity $h_{50\%}$ is the indicator of the safeness of the material, and it shows how the material responds to external stimuli such as shock and friction. It is measured in terms of drop height that is the height from which fifty percent of the drops result in the reaction of the sample (Rice & Hare, 2002); and the higher the value of $h_{50\%}$, the lower the impact sensitivity (Mei *et al*., 2019). It is expected that the best material will have moderate sensitivity which is comparable to that of common explosives. The computed impact sensitivities of all designed compounds range from 30 to 33 cm, that is comparable to those of common energetic materials HMX (32 cm) and RDX (28 cm).

The degree of self-oxidation α of the compound indicates the ability of the material to detonate and associated with the content of oxidant, oxygen and fluorine in this case. The higher value of α indicates that the material is more feasible for self-oxidation. For the compounds A-G, the values of α obtained by equation (25) are between 0.92 and 1.17 (Table 7). Compounds C, D, E, F, and G have coefficients of oxidation greater or equal to one, which is acceptable for HEDM.

Overall, among newly designed compounds, B and D exhibit improved energetic properties compared to other fluorinated triazoles as well as original compound A. Regarding most informative properties, the detonation heat, velocity and pressure, the compounds B and D are predicted to be on the top of the rank. It is suppose that, their enhanced energetic characteristics relate to the structural features, namely, fluorination of the hydrazine chain. At the same time, the fluorination of the triazole rings impairs the properties.

CHAPTER FIVE

CONCLUSION AND RECOMENDATIONS

5.1 Conclusion

In this study, fluorinated HEDM were designed by introducing fluorine atoms into original bridged trinitromethyl azo triazoles molecule to obtain mono-, di-, tri- and tetrafluorinated species. Molecular geometries, infrared spectra, frontier molecular orbitals, thermodynamic and energetic properties were computed and analyzed. The position and number of fluorine substituents resulted in a noticeable change in the enthalpies of formation of gaseous and solid compounds. Generally, introduction of the F atoms into azo linkage brings to an elevation of energetic properties while the triazole ring fluorination lowers the detonation characteristics. Among the designed triazoles, the species with only fluorinated hydrazine chain may be regarded as potential candidates of HEDM with advanced energetic properties compared to common explosives. The results provide basic information for invention and synthesis of novel energetic materials.

5.2 Recommendations

Highly nitrated energetic materials have been investigated by using quantum chemical methods and found to release high energy compared to traditional explosives. The challenge of these materials is their sensitivities which makes them environmentally unfriendly and complex synthesis methods. In this regard, the design of new fluorinated materials with different number and position of fluorine atoms on the bridged trinitromethyl triazole framework were proposed. The properties computed for azo fluorination show the improvement in performance of the material while ring fluorination shows no any improvement but still further studies are recommended as follows:

(i) Investigation of the mechanism of azo and ring fluorination on the triazole framework.

(ii) Computational studies on tris, tetra and higher aromatic ring energetic compounds and their derivatives are also recommended.

(iii) Further studies on the influence of theoretical approach on the results, for instance using different DFT functionals, effect of dispersion energy and excited states.

REFERENCES

Adolph, H., Holden, J., & Cichra, D. (1981). *Technical Report NSWC*. Naval Surface Weapons Center, Dahlgren, VA. https://www.worldcat.org.

Agrawal, H., & Mishra, A. K. (2017). A study on influence of density and viscosity of emulsion explosive on its detonation velocity. *Modelling, Measurement and Control*, *78*, 316-336. https://scholar.google.com/scholar?cluster=16334065300104089010&hl = en&as_sdt=0,5.

Ainsworth, C., & Jones, R. (1955). Isomeric and Nuclear-substituted β-Aminoethyl-1, 2, 4-triazoles. *Journal of the American Chemical Society*, *77*(3), 621-624. https://doi.org/ 10.1021 /ja01608a028.

Ali, S., Banck, M., Braithwaite, R., Bunt, J., Curtis, D., Fox, N., Hanwell, M., Hutchison, G., Benoit, J., & Lonie, D. (2012). Avogadro: An open-source molecular builder and visualization tool, version 1.0. 3. https://doi.org/10.1021/acs.molpharmaceut.7b00068.

Babkin, V., Korzhavin, A., & Bunev, V. (1991). Propagation of premixed gaseous explosion flames in porous media. *Combustion and Flame*, *87*(2), 182-190. https://doi.org/ 10.1016/ 0010-2180(91)90168-B.

Becke, A. D. (1993). A new mixing of Hartree–Fock and local density-functional theories. *Journal of Chemical Physics*, *98*(2), 1372-1377. https://doi.org/10.1063/1.464304.

Bendezu, M., Romanel, C., & Roehl, D. (2017). Finite element analysis of blast-induced fracture propagation in hard rocks. *Computers & Structures*, *182*, 1-13. https:// doi.org/ 10.1016/ j.compstruc.2016.11.006.

Bowden, F. P., & Yoffe, A. D. (1985). *Initiation and Growth of Explosion in Liquids and Solids*. CUP Archive. https://b-ok.africa/s/?q=Bowden.

Brinck, T. (2014). *Introduction to Green Energetic Materials*. Wiley Online Library. https://doi.org/10.1002/9781118676448.

Byrd, E. F., & Rice, B. M. (2006). Improved prediction of heats of formation of energetic materials using quantum mechanical calculations. *The Journal of Physical Chemistry A*, *110*(3), 1005-1013. https://doi.org/10.1021/jp0536192.

Cawkwell, M. J., & Manner, V. W. (2019). Ranking the drop-weight impact sensitivity of common explosives using Arrhenius chemical rates computed from quantum molecular dynamics simulations. *The Journal of Physical Chemistry A*, *124*(1), 74-81. https://doi.org/10.1021/acs.jpca.9b10808.

Chavez, D. E., Hanson, S. K., Veauthier, J. M., & Parrish, D. A. (2013). Electroactive Explosives: Nitrate Ester-Functionalized 1, 2, 4, 5-Tetrazines. *Angewandte Chemie*, *125*(27), 7014-7017. https://doi.org/10.1002/ange.201302128.

Chavez, D. E., Tappan, B. C., Mason, B. A., & Parrish, D. (2009). Synthesis and Energetic Properties of Bis-(Triaminoguanidinium) 3, 3′-Dinitro-5, 5′-Azo-1, 2, 4-Triazolate (TAGDNAT): A New High-Nitrogen Material. *Propellants, Explosives, Pyrotechnics: An International Journal Dealing with Scientific and Technological Aspects of Energetic Materials*, *34*(6), 475-479. https://doi.org/10.1002/prep. 200800081.

Collins, E. S., & Gottfried, J. L. (2017). Laser-induced Deflagration for the Characterization of Energetic Materials. *Propellants, Explosives, Pyrotechnics*, *42*(6), 592-602. https://doi.org/10.1002/prep.201700040.

Dalinger, I. L., Kormanov, A. V., Suponitsky, K. Y., Muravyev, N. V., & Sheremetev, A. B. (2018). Pyrazole–Tetrazole Hybrid with Trinitromethyl, Fluorodinitromethyl, or (Difluoroamino) dinitromethyl Groups: High-Performance Energetic Materials. *Chemistry–An Asian Journal*, *13*(9), 1165-1172. https://doi.org/10.1002/asia. 201800214.

Dharavath, S., Zhang, J., Imler, G. H., Parrish, D. A., & Jean'ne, M. S. (2017). 5-(Dinitromethyl)-3-(trinitromethyl)-1, 2, 4-triazole and its derivatives: A new application of oxidative nitration towards gem-trinitro-based energetic materials. *Journal of Materials Chemistry A*, *5*(10), 4785-4790. https://doi.org/10.1039/ C7TA00730B.

Diegelmann, F., Hickel, S., & Adams, N. A. (2016). Shock Mach number influence on reaction wave types and mixing in reactive shock–bubble interaction. *Combustion and Flame*, *174*, 85-99. https://doi.org/10.1016/j.combustflame.2016.09.014.

Espinosa, E., Souhassou, M., Lachekar, H., & Lecomte, C. (1999). Topological analysis of the electron density in hydrogen bonds. *Acta Crystallographica Section B: Structural Science*, *55*(4), 563-572. https://doi.org/10.1107/S0108768199002128.

Feng, Y., Bi, Y., Zhao, W., & Zhang, T. (2016). Anionic metal–organic frameworks lead the way to eco-friendly high-energy-density materials. *Journal of Materials Chemistry A*, *4*(20), 7596-7600. https://doi.org/10.1039/C6TA02340A.

Fischer, D., Klapötke, T. M., Piercey, D. G., & Stierstorfer, J. (2013). Synthesis of 5-Aminotetrazole-1 N-oxide and Its Azo Derivative: A Key Step in the Development of New Energetic Materials. *Chemistry–A European Journal*, *19*(14), 4602-4613. https://doi.org/ 10.1002/chem.201203493.

Fischer, N., Fischer, D., Klapötke, T. M., Piercey, D. G., & Stierstorfer, J. (2012). Pushing the limits of energetic materials–the synthesis and characterization of dihydroxylammonium 5, 5′-bistetrazole-1, 1′-diolate. *Journal of Materials Chemistry*, *22*(38), 20418-20422. https://doi.org/10.1039/C2JM33646D.

Fischer, N., Karaghiosoff, K., Klapötke, T. M., & Stierstorfer, J. (2010). New Energetic Materials featuring Tetrazoles and Nitramines–Synthesis, Characterization and Properties. *Zeitschrift fur Anorganische und Allgemeine Chemie*, *636*(5), 735-749. https://doi.org/10.1002/zaac.200900521.

Fried, L. E., & Ruggiero, A. J. (1994). Energy transfer rates in primary, secondary, and insensitive explosives. *The Journal of Physical Chemistry*, *98*(39), 9786-9791. https://doi.org/10.1021/j100090a012.

Frisch, M., Trucks, G., Schlegel, H., Scuseria, G., Robb, M., Cheeseman, J., Scalmani, G., Barone, V., Mennucci, B., & Petersson, G. (2009). Gaussian 09; Gaussian, Inc. *Wallingford, CT*, *32*, 5648-5652. https://ci.nii.ac.jp/naid/ 10029868106.

Fu, W., Zhao, B., Zhang, M., Li, C., Gao, H., Zhang, J., & Zhou, Z. (2017). 3, 4-Dinitro-1-(1 H-tetrazol-5-yl)-1 H-pyrazol-5-amine (HANTP) and its salts: Primary and secondary explosives. *Journal of Materials Chemistry A*, *5* (10), 5044-5054. https://doi.org/ 10.1039/C6TA08376E.

Gao, H., Zhou, Y., & Jean'ne, M. S. (2020). Dinitromethyl groups enliven energetic salts. *Energetic Materials Frontiers*. https://doi.org/10.1016/j.enmf.2020.04.001.

Gardiner, W. C., & Burcat, A. (1984). *Combustion Chemistry*. Springer. https://doi.org/ 10.1007/ 978-1-4684-0186-8.

Gibson, H. W. (1969). Chemistry of formic acid and its simple derivatives. *Chemical Reviews, 69*(5), 673-692. https://doi.org/10.1021/cr60261a005.

Gilman, J. J. (1995). Chemical reactions at detonation fronts in solids. *Philosophical Magazine B, 71*(6), 1057-1068. https://doi.org/10.1080/01418639508241895.

Gu, B. M., Lin, H., & Zhu, S. G. (2014). Ab initio studies of 1, 3, 5, 7-tetranitro-1, 3, 5, 7-tetrazocine/1, 3-dimethyl-2-imidazolidinone cocrystal under high pressure using dispersion corrected density functional theory. *Journal of Applied Physics*, *115*(14), 143509. https://doi.org/10.1063/1.4871398.

Gurvich, L., Yungman, V., Bergman, G., Veitz, I., Gusarov, A., Iorish, V., Leonidov, V. Y., Medvedev, V., Belov, G., & Aristova, N. (1992). *Thermodynamic Properties of Individual Substances. Ivtanthermo for Windows Database on Thermodynamic Properties of Individual Substances and Thermodynamic Modeling Software. Version 3.0 (Glushko Thermocenter of RAS, Moscow, 1992-2000)*. https://doi.org/10.11648/ j.ijct.20150306.13.

Haiges, R., & Christe, K. O. (2013). Energetic high-nitrogen compounds: 5-(trinitromethyl)-2 H-tetrazole and-tetrazolates, preparation, characterization, and conversion into 5-(dinitromethyl) tetrazoles. *Inorganic Chemistry*, *52*(12), 7249-7260. https://doi.org/ 10.1021/ic400919n.

He, C., & Shreeve, J. M. (2016). Potassium 4, 5-Bis (dinitromethyl) furoxanate: A Green Primary Explosive with a Positive Oxygen Balance. *Angewandte Chemie*, *128*(2), 782-785. https://doi.org/10.1002/ange.201509209.

He, P., Mei, H., Yang, J., & Zhang, J. (2019). Design and properties of a new family of bridged bis (nitraminotetrazoles) as promising energetic materials. *New Journal of Chemistry*, *43*(10), 4235-4241. https://doi.org/10.1039/C8NJ05633A.

He, P., Zhang, J. G., Wang, K., Yin, X., & Zhang, T. L. (2015). Combination multinitrogen with good oxygen balance: molecule and synthesis design of polynitro-substituted tetrazolotriazine-based energetic compounds. *The Journal of Organic Chemistry*, *80*(11), 5643-5651. https://doi.org/10.1021/acs.joc.5b00545.

He, P., Zhang, J., & Wu, J. (2019). DFT studies on new family of high-energy density energetic bis (trinitromethyl) azo tetrazoles and triazoles. *Journal of Physical Organic Chemistry*, *32*(7), e3953. https://doi.org/10.1002/poc.3953.

Hervé, G., Roussel, C., & Graindorge, H. (2010). Selective Preparation of 3, 4, 5-Trinitro-1H-Pyrazole: A Stable All-Carbon-Nitrated Arene. *Angewandte Chemie International Edition*, *49*(18), 3177-3181. https://doi.org/10.1002/anie.201000764.

Holl, G., Klapötke, T. M., Polborn, K., & Rienäcker, C. (2003). Structure and bonding in 2-Diazo-4, 6-dinitrophenol (DDNP). *Propellants, Explosives, Pyrotechnics: An International Journal Dealing with Scientific and Technological Aspects of Energetic Materials*, *28*(3), 153-156. https://doi.org/10.1002/prep.200390022.

Holm, S. C., & Straub, B. F. (2011). Synthesis of n-substituted 1, 2, 4-triazoles. *Organic Preparations and Procedures International*, *43*(4), 319-347. https://doi.org/ 10.1080/00304948.2011.593999.

Jin, X., Hu, B., Jia, H., Liu, Z., & Lu, C. (2014). Dft theoretical study of energetic nitrogen-rich $C_4N_6H_8$-n(NO_2)n derivatives. *Quimica Nova*, *37*(1), 74-80. https://doi.org/10. 1590/S0100 /40422014000100014.

Kamlet, M., & Adolph, H. (1979). The relationship of impact sensitivity with structure of organic high explosives. Polynitroaromatic explosives. *Propellants, Explosives, Pyrotechnics*, *4*(2), 30-34. https://doi.org/10.1002/prep.19790040204.

Kamlet, M. J., & Hurwitz, H. (1968). Chemistry of detonations. Evaluation of a simple predictional method for detonation velocities of C–H–N–O explosives. *The Journal of Chemical Physics*, *48*(8), 3685-3692. https://doi.org/10.1063/1.1669671.

Kamlet, M. J., & Jacobs, S. (1968). Chemistry of detonations. A simple method for calculating detonation properties of C–H–N–O explosives. *The Journal of Chemical Physics*, *48*(1), 23-35. https://doi.org/10.1063/1.1667908.

Kamlet, M. J., & Short, J. M. (1980). The chemistry of detonations. A “rule for gamma” as a criterion for choice among conflicting detonation pressure measurements. *Combustion and Flame, 38*, 221-230. https://doi.org/10.1016/0010-2180(80)90055-3.

Karaghiosoff, K., Klapötke, T. M., Michailovski, A., Nöth, H., Suter, M., & Holl, G. (2003). 1, 4-Diformyl-2, 3, 5, 6-Tetranitratopiperazine: A New Primary Explosive Based on Glyoxal. *Propellants, Explosives, Pyrotechnics: An International Journal Dealing with Scientific and Technological Aspects of Energetic Materials*, *28*(1), 1-6. https://doi.org/10.1002/prep.200390002.

Keshavarz, M. H. (2005). A simple approach for determining detonation velocity of high explosive at any loading density. *Journal of Hazardous Materials, 121*(1-3), 31-36. https://doi.org/10.1016/j.jhazmat.2005.01.028.

Keshavarz, M. H. (2007). A simple theoretical prediction of detonation velocities of non-ideal explosives only from elemental composition. *New Research on Hazardous Materials 12*(3), 293-310. Nova Science Publishers, Inc. https://books.google.co.tz/books.

Keshavarz, M. H. (2008). Estimating heats of detonation and detonation velocities of aromatic energetic compounds. *Propellants, Explosives, Pyrotechnics: An International Journal Dealing with Scientific and Technological Aspects of Energetic Materials*, *33*(6), 448-453. https://doi.org/10.1002/prep.200800226.

Keshavarz, M. H., & Pouretedal, H. R. (2004). An empirical method for predicting detonation pressure of CHNOFCl explosives. *Thermochimica Acta*, *414*(2), 203-208. https://doi.org/ 10.1016/ j.tca.2003.11.019.

Keshavarz, M. H., Pouretedal, H. R., & Semnani, A. (2007). Novel correlation for predicting impact sensitivity of nitroheterocyclic energetic molecules. *Journal of Hazardous Materials, 141*(3), 803-807. https://doi.org/10.1016/j.jhazmat.2006.07.046.

Kettner, M., & Klapötke, T. M. (2014). 5, 5′-Bis-(trinitromethyl)-3, 3′-bi-(1, 2, 4-oxadiazole): a stable ternary CNO-compound with high density. *Chemical Communications, 50*(18), 2268-2270. https://doi: 10.1039/C3CC49879D.

Kharb, R., Sharma, P. C., & Yar, M. S. (2011). Pharmacological significance of triazole scaffold. *Journal of Enzyme Inhibition and Medicinal Chemistry*, *26*(1), 1-21. https://doi.org/ 10.3109/14756360903524304.

Klapötke, T. M. (2019). *Chemistry of High Energy Materials*. Walter de Gruyter GmbH & Co KG. https://doi.org/10.1515/9783110273595.

Kotomin, A., Dushenok, S., & Ilyushin, M. (2017). Detonation velocity of highly dispersed ammonium perchlorate and its mixtures with explosive substances. *Combustion, Explosion, and Shock Waves*, *53*(3), 353-357. https://doi.org/10.1134/S001050821 7030145.

Kovalev, E., & Postovskii, I. Y. (1971). Investigations in the 1, 2, 4-triazole series. *Chemistry of Heterocyclic Compounds*, *4*(4), 544-545. https://doi.org/10.1007/BF00486784.

Lakhan, R., & Ternai, B. (1974). Advances in oxazole chemistry. In R. Lakhan & B. Ternai (Eds). *Advances in Heterocyclic Chemistry*, 17(3), 99-211. Elsevier. https://doi.org/ 10. 1016/S0065-2725(08)60908-3.

Licht, H. H. (2000). Performance and sensitivity of explosives. *Propellants, Explosives, Pyrotechnics*, *25*(3), 126-132. https://doi.org/10.1002/1521-4087.

Liu, Y., He, C., Tang, Y., Imler, G. H., Parrish, D. A., & Jean'ne, M. S. (2019). Tetrazolyl and dinitromethyl groups with 1, 2, 3-triazole lead to polyazole energetic materials. *Dalton Transactions*, *48*(10), 3237-3242. https://doi.org/10.1039/C8DT05071F.

Lu, T., & Chen, F. (2012). Multiwfn: A multifunctional wavefunction analyzer. *Journal of Computational Chemistry*, *33*(5), 580-592. https://doi.org/10.1002/jcc.22885.

Luan, F., Liu, H., Wen, Y., Li, Q., Zhang, X., & Sun, J. (2010). QSPR Study for Estimation of Density of Some Aromatic Explosives by Multiple Linear Regression Approach. *Propellants, Explosives, Pyrotechnics*, *35*(2), 169-174. https://doi.org/10.1002/ prep.200800091.

Martinez, H., Zheng, Z., & Dolbier Jr, W. R. (2012). Energetic materials containing fluorine. Design, synthesis and testing of furazan-containing energetic materials bearing a

pentafluorosulfanyl group. *Journal of Fluorine Chemistry*, *14*(3), 112-122. https:// doi.org/ 10.1016/j.jfluchem.2012.03.010.

McNesby, K., & Coffey, C. (1997). Spectroscopic determination of impact sensitivities of explosives. *Journal of Physical Chemistry B*, *101*(16), 3097-3104. https://doi.org/10. 1021/jp961771.

Mertuszka, P., Cenian, B., Kramarczyk, B., & Pytel, W. (2018). Influence of explosive charge diameter on the detonation velocity based on Emulinit 7L and 8L bulk emulsion explosives. *Central European Journal of Energetic Materials*, *15*(2), 13-21. https://doi: 10.22211/cejem/78090.

Michalchuk, A. A., Trestman, M., Rudić, S., Portius, P., Fincham, P. T., Pulham, C. R., & Morrison, C. A. (2019). Predicting the reactivity of energetic materials: An ab initio multi-phonon approach. *Journal of Materials Chemistry A*, *7*(33), 39-53. https://doi: 10.1039/C9TA06209B.

Millar, D. I. (2011). *Energetic Materials at Extreme Conditions*. Springer Science & Business Media. https://doi: 10.1007/978-3-642-23132-2.

Mishra, A. K., Agrawal, H., & Raut, M. (2019). Effect of aluminum content on detonation velocity and density of emulsion explosives. *Journal of Molecular Modeling*, *25*(3), 1-5. https://doi.org/10.1007/s00894-019-3961-3.

Mullay, J. (1987a). A relationship between impact sensitivity and molecular electronegativity. *Propellants, Explosives, Pyrotechnics*, *12*(2), 60-63. https://doi.org/ 10.1002/prep. 19870120206.

Mullay, J. (1987b). Relationships between impact sensitivity and molecular electronic structure. *Propellants, Explosives, Pyrotechnics*, *12*(4), 121-124. https://doi.org/10. 1002/ prep. 19870120403.

Murray, J. S., Lane, P., & Politzer, P. (1995). Relationships between impact sensitivities and molecular surface electrostatic potentials of nitroaromatic and nitroheterocyclic molecules. *Molecular Physics*, *85*(1), 1-8. https://doi.org/10.1080/002689795001008.

Murray, J. S., Lane, P., Politzer, P., & Bolduc, P. R. (1990). A relationship between impact sensitivity and the electrostatic potentials at the midpoints of C_nNO_2 bonds in nitroaromatics. *Chemical Physics Letters, 168*(2), 135-139. https://doi.org/10.1016/0009-2614(90)85118-V.

Olah, G. A., & Squire, D. R. (2012). *Chemistry of Energetic Materials*. Academic press. https://books.google.co.tz/books?hl=en&lr=&id=ZUw7_ TTKDjoC&oi = fnd&pg.

Onyelowe, K., Buivan, D., Orji, F., Nguyen, M., Igboayaka, C., & Ugwuanyi, H. (2018). Exploring rock by blasting with gunpowder as explosive, aggregate production and quarry dust utilization for construction purposes. *Oklahoma State University Electronic Journal of Geotechnical Engineering, 23(4)*, 447-456. https://scholar.google.com/scholar?cluster=10593708956326950 66&hl=en&as_sdt.

Ostrovskii, V., Popova, E., & Trifonov, R. (2017). Developments in tetrazole chemistry (2009–16). *Advances in Heterocyclic Chemistry*, 12(3), 1-62. Elsevier. https://doi.org/10.1016/bs.aihch.2016.12.003.

Owens, F. J., Jayasuriya, K., Abrahmsen, L., & Politzer, P. (1985). Computational analysis of some properties associated with the nitro groups in polynitroaromatic molecules. *Chemical Physics Letters*, *116*(5), 434-438. https://doi.org/10.1016/0009-2614(85)80199-8.

Palysaeva, N. V., Gladyshkin, A. G., Vatsadze, I. A., Suponitsky, K. Y., Dmitriev, D. E., & Sheremetev, A. B. (2019). N-(2-Fluoro-2, 2-dinitroethyl) azoles: A novel assembly of diverse explosophoric building blocks for energetic compound design. *Organic Chemistry Frontiers, 6*(2), 249-255. https://doi.org/10.1039/C8QO01173G.

Perger, W. (2003). Calculation of band gaps in molecular crystals using hybrid functional theory. *Chemical Physics Letters*, *368*(3-4), 319-323. https://doi.org/10.1016/S0009-2614(02)01879-1.

Petree, H. E., Pociask, J. R., & Gupton, J. T. (1981). Method for direct preparation for 1, 2, 4-triazole from hydrazine and formamide. *Acta Crystallographica Section C: Crystal Structure Communications*, *53*(11), 1621-1622. http://scholarship.richmond.edu/chemistry-facultypublications.

Politzer, P., Abrahmsen, L., & Sjoberg, P. (1984). Effects of amino and nitro substituents upon the electrostatic potential of an aromatic ring. *Journal of the American Chemical Society*, *106*(4), 855-860. https://doi.org/10.1021/ja00316a005.

Politzer, P., Landry, S. J., & Waernheim, T. (1982). Proposed procedure for using electrostatic potentials to predict and interpret nucleophilic processes. *The Journal of Physical Chemistry*, *86*(24), 4767-4771. https://doi.org/10.1021/j100221a024.

Politzer, P., Martinez, J., Murray, J. S., Concha, M. C., & Toro-Labbé, A. (2009). An electrostatic interaction correction for improved crystal density prediction. *Molecular Physics*, *107*(19), 2095-2101. https://doi.org/10.1080/00268970903156306.

Politzer, P., & Murray, J. S. (2011). Some perspectives on estimating detonation properties of C, H, N, O compounds. *Central European Journal of Energetic Materials*, *8*(3), 209-220. http://yadda.icm.edu.pl/yadda/element/bwmeta1.element.baztech-article-BAT1-0040 - 0019.

Politzer, P., & Murray, J. S. (2015). Impact sensitivity and the maximum heat of detonation. *Journal of Molecular Modeling*, *21*(10), 262. https://doi.org/10.1007/s00894-015-2793-z.

Politzer, P., Murray, J. S., Edward Grice, M., Desalvo, M., & Miller, E. (1997). Calculation of heats of sublimation and solid phase heats of formation. *Molecular Physics*, *91*(5), 923-928. https://www.tandfonline.com/doi/abs/10.1080/002689797171030.

Politzer, P., Murray, J. S., Seminario, J. M., Lane, P., Grice, M. E., & Concha, M. C. (2001). Computational characterization of energetic materials. *Journal of Molecular Structure: Theoretical Chemistry*, *573*(1-3), 1-10. https://doi.org/10.1016/S0166-1280(01)00533-4.

Poludnenko, A. Y., Chambers, J., Ahmed, K., Gamezo, V. N., & Taylor, B. D. (2019). A unified mechanism for unconfined deflagration-to-detonation transition in terrestrial chemical systems and type supernovae. *Science*, *366*(6), 1-9. https://doi.org/10.1126/science.aau7365.

Potts, K. (1961). The Chemistry of 1, 2, 4-Triazoles. *Chemical Reviews*, *61*(2), 87-127. https://doi.org/10.1021/cr60210a001.

Remennikov, A., Ngo, T., Mohotti, D., Uy, B., & Netherton, M. (2017). Experimental investigation and simplified modeling of response of steel plates subjected to close-in blast loading from spherical liquid explosive charges. *International Journal of Impact Engineering*, *101*, 78-89. https://doi.org/10.1016/j.ijimpeng.2016.11.013.

Rice, B. M., Byrd, E. F., & Mattson, W. D. (2007). Computational Aspects of Nitrogen-rich HEDMs. In M. K. Thomas (Ed). *High Energy Density Materials* (pp. 153-194). Springer. https://doi.org/ 10.1007/430_2006_053.

Rice, B. M., & Hare, J. J. (2002). A quantum mechanical investigation of the relation between impact sensitivity and the charge distribution in energetic molecules. *The Journal of Physical Chemistry A*, *106*(9), 1770-1783. https://doi.org/10.1021/ jp012602q.

Rice, B. M., Pai, S. V., & Hare, J. (1999). Predicting heats of formation of energetic materials using quantum mechanical calculations. *Combustion and Flame*, *118*(3), 445-458. https://doi.org/10.1016/S0010-2180(99)00008-5.

Schultz, E., & Shepherd, J. (2000). Validation of detailed reaction mechanisms for detonation simulation. *Journal of KONES*, *9*(3), 1-2. https://resolver.caltech.edu/Caltech:1999. 005.

Semenov, V., Kanischev, M., Shevelev, S., & Kiselyov, A. (2009). Thermal ring-opening reaction of N-polynitromethyl tetrazoles: facile generation of nitrilimines and their reactivity. *Tetrahedron*, *65*(17), 3441-3445. https://doi.org/10.1016/j.tet.2009.02.032.

Semenov, V. V., Shevelev, S. A., Bruskin, A. B., Shakhnes, A. K., & Kuz'min, V. S. (2017). Synthesis of 5, 5'-dinitro-2, 2'-bis (polynitromethyl)-bi (1, 2, 3 (4)-triazoles), hydrogen-free oxidizers. *Chemistry of Heterocyclic Compounds*, *53*(6-7), 728-732. https://doi.org/ 10.1007/s10593-017-2117-6.

Sheremetev, A. B., Palysaeva, N. V., Struchkova, M. I., Suponitsky, K. Y., & Antipin, M. Y. (2012). Copper-Catalyzed C–N Coupling Reactions of Nitrogen-Rich Compounds– Reaction of Iodofurazans with s-Tetrazinylamines. *European Journal of Organic Chemistry*, *2012*(11), 2266-2272. https://doi.org/10.1002/ejoc.201101732.

Shtertser, A., Rybin, D., Ulianitsky, V. Y., Park, W., Datekyu, M., Wada, T., & Kato, H. (2020). Characterization of nanoscale detonation carbon produced in a pulse gas-detonation device. *Diamond and Related Materials*, *101*(2), 107553. https://doi.org/10.1016/ j.diamond.2019.107553.

Sjoberg, P., & Politzer, P. (1990). Use of the electrostatic potential at the molecular surface to interpret and predict nucleophilic processes. *Journal of Physical Chemistry*, *94*(10), 3959-3961. https://doi.org/10.1021/j100373a017.

Smirnov, A., Lempert, D., Pivina, T., & Khakimov, D. (2011). Basic Characteristics for Estimation Polynitrogen Compounds Effciency. *Central European Journal of Energetic Materials*, *8*(4), 233-247. http://yadda.icm.edu.pl/baztech/element/bmeta1. element.baztech-article-BAT1-0040-0021.

Sun, Q., Li, X., Lin, Q., & Lu, M. (2019). Dancing with 5-substituted monotetrazoles, oxygen-rich ions, and silver: towards primary explosives with positive oxygen balance and excellent energetic performance. *Journal of Materials Chemistry A*, *7*(9), 4611-4618. https://doi.org/10.1039/C8TA12506F.

Talawar, M., Sivabalan, R., Mukundan, T., Muthurajan, H., Sikder, A., Gandhe, B., & Rao, A. S. (2009). Environmentally compatible next generation green energetic materials (GEMs). *Journal of Hazardous Materials*, *161*(3), 589-607. https://doi.org/10.1016/ j.jhazmat.2008.04.011.

Tarver, C. (1982a). Chemical energy release in one-dimensional detonation waves in gaseous explosives. *Combustion and Flame*, *46*(3), 111-133. https://doi.org/10.1016/0010-2180(82)90011-6.

Tarver, C. (1982b). Chemical energy release in self-sustaining detonation waves in condensed explosives. *Combustion and Flame*, *46*(4), 157-176. https://doi.org/10. 1016/0010-2180(82)90013-X.

Tarver, C. M. (2020). Jones–Wilkins–Lee unreacted and reaction product equations of state for overdriven detonations in octogen-and triaminotrinitrobenzene-based plastic-bonded explosives. *The Journal of Physical Chemistry A*, *124*(7), 1399-1408. https://doi.org/ 10.1021/acs.jpca.9b10804.

Thottempudi, V., Forohor, F., Parrish, D. A., & Shreeve, J. M. (2012). Tris (triazolo) benzene and Its Derivatives: High-Density Energetic Materials. *Angewandte Chemie International Edition*, *51*(39), 9881-9885. https://doi.org/10.1002/anie.201205134.

Thottempudi, V., & Shreeve, J. M. (2011). Synthesis and Promising Properties of a New Family of High-Density Energetic Salts of 5-Nitro-3-trinitromethyl-1 H-1, 2, 4-triazole and 5, 5′-Bis (trinitromethyl)-3, 3′-azo-1 H-1, 2, 4-triazole. *Journal of the American Chemical Society*, *133*(49), 19982-19992. https://doi.org/10.1021/ja208990z.

Tokarev, K. (2007). *OpenThermo Version.1.0 Beta 1 (C) ed. 2007-2009*. http://openthermo.software.informer.com/.

Türker, L. (2016). Azo-bridged triazoles: Green energetic materials. *Defence Technology*, *12*(1), 1-15. https://doi.org/10.1016/j.dt.2015.11.002.

Walters, I. V., Journell, C. L., Lemcherfi, A., Gejji, R. M., Heister, S. D., & Slabaugh, C. D. (2020). Operability of a Natural Gas–Air Rotating Detonation Engine. *Journal of Propulsion and Power*, *36*(3), 453-464. https://doi.org/10.2514/1.B37735.

Wang, G., Xiao, H., Ju, X., & Gong, X. (2006). Calculation of detonation velocity, pressure, and electric sensitivity of nitro arenes based on quantum chemistry. *Propellants, Explosives, Pyrotechnics: An International Journal Dealing with Scientific and Technological Aspects of Energetic Materials*, *31*(5), 361-368. https://doi.org/10.1002/prep.200600049.

Wei, T., Zhu, W., Zhang, X., Li, Y.F., & Xiao, H. (2009). Molecular design of 1, 2, 4, 5-tetrazine-based high-energy density materials. *The Journal of Physical Chemistry A*, *113*(33), 9404-9412. https://doi.org/10.1021/jp902295v.

Wilson, W. S., Bliss, D. E., Christian, S. L., & Knight, D. J. (1990). *Explosive Properties of Polynitroaromatics*. Naval Weapons Center China Lake CA. https://apps.dtic.mil/sti/pdfs/ADA229627.

Wu, Q., Zhu, W., & Xiao, H. (2013). Molecular design of tetrazole-and tetrazine-based high-density energy compounds with oxygen balance equal to zero. *Journal of Chemical and Engineering Data*, *58*(10), 2748-2762. https://doi.org/10.1021/je4004367.

Wu, Q., Zhu, W., & Xiao, H. (2014). A new design strategy for high-energy low-sensitivity explosives: combining oxygen balance equal to zero, a combination of nitro and amino groups, and N-oxide in one molecule of 1-amino-5-nitrotetrazole-3 N-oxide. *Journal of Materials Chemistry A*, *2*(32), 13006-13015. https://doi.org/10.1039/C4TA01879F.

Yan, Q. L., & Zeman, S. (2013). Theoretical evaluation of sensitivity and thermal stability for high explosives based on quantum chemistry methods. *International Journal of Quantum Chemistry*, *113*(8), 1049-1061. https://doi.org/10.1002/qua.24209.

Yang, J., Gong, X., Mei, H., Li, T., Zhang, J., & Gozin, M. (2018). Design of zero oxygen balance energetic materials on the basis of Diels–Alder chemistry. *The Journal of Organic Chemistry*, *83*(23), 14698-14702. https://doi.org/10.1021/acs.joc.8b02000.

Ye, C., Gard, G. L., Winter, R. W., Syvret, R. G., Twamley, B., & Shreeve, J. n. M. (2007). Synthesis of pentafluorosulfanylpyrazole and pentafluorosulfanyl-1, 2, 3-triazole and their derivatives as energetic materials by click chemistry. *Organic Letters*, *9*(19), 3841-3844. https://doi.org/10.1021/ol701602a.

Ye, C., Xiao, J. C., Twamley, B., & Jean'ne, M. S. (2005). Energetic salts of azotetrazolate, iminobis (5-tetrazolate) and 5, 5′-bis (tetrazolate). *Chemical Communications*, *21*(5), 50-56. https://doi.org/10.1039/B502583D.

Yuan, W., Su, X., Wang, W., Wen, L., & Chang, J. (2019). Numerical study of the contributions of shock wave and detonation gas to crack generation in deep rock without free surfaces. *Journal of Petroleum Science and Engineering*, *177*, 699-710. https://doi.org/10. 1016/j.petrol.2019.02.004.

Yunoshev, A., Plastinin, A., & Rafeichik, S. (2017). Detonation velocity of an emulsion explosive sensitized with polymer microballoons. *Combustion, Explosion, and Shock Waves*, *53*(6), 738-743. https://doi.org/10.1134/S0010508217060168.

Zeman, S., & Jungová, M. (2016). Sensitivity and performance of energetic materials. *Propellants, Explosives, Pyrotechnics*, *41*(3), 426-451. https://doi.org/10.1002/prep.201500351.

Zhang, F., Gerrard, K., & Ripley, R. C. (2009). Reaction mechanism of aluminum-particle-air detonation. *Journal of Propulsion and Power*, *25*(4), 845-858. https://doi.org/10.2514/1.41707.

Zhang, J., Liu, Y., Zhou, J., Bi, F., & Wang, B. (2019). Effect of Fluoro Substituents on Polynitroarylenes: Design, Synthesis and Theoretical Studies of Fluorinated Nitrotoluenes. *Chemistry Europe*, *84*(1), 92-97. https://doi.org/10.1002/cplu.201800523.

Zhurko, G., & Zhurko, D. (2015). *Chemcraft Graphical Program for Visualization of Computed Results. Version 1.7 (build 365)*. https://doi.org/10.1134/S0030400130401.

APPENDICES

Appendix 1: Optimized Cartesian coordinates (in Å) of atoms in compound A

No	Atomic number	Atomic type	X	Y	Z
1	6	O	–4.101	–0.203	0.643
2	7	N	–4.962	–1.078	1.085
3	7	N	–4.300	–2.287	1.221
4	6	C	–3.058	–2.115	0.857
5	7	N	–2.864	–0.801	0.478
6	7	N	–1.758	–0.109	0.067
7	7	N	–0.765	–0.850	–0.067
8	7	N	0.341	–0.159	–0.477
9	6	C	0.534	1.156	–0.856
10	7	N	1.776	1.328	–1.220
11	7	N	2.438	0.119	–1.084
12	6	C	1.577	–0.756	–0.643
13	6	C	1.860	–2.184	–0.355
14	7	N	3.252	–2.584	–0.908
15	7	N	0.789	–3.101	–1.009
16	7	N	1.876	–2.526	1.158
17	8	O	4.181	–2.083	–0.309
18	8	O	3.266	–3.345	–1.855
19	8	O	1.211	–1.789	1.869
20	8	O	0.484	–2.783	–2.142
21	6	C	–4.383	1.225	0.354
22	7	N	–5.775	1.625	0.907
23	7	N	–4.399	1.567	–1.158
24	8	O	–5.041	2.545	–1.478
25	8	O	–3.734	0.829	–1.869
26	8	O	–6.704	1.124	0.309
27	1	H	–2.276	–2.859	0.843
28	7	N	–3.313	2.142	1.009
29	8	O	–2.890	3.068	0.342
30	8	O	–3.008	1.824	2.142
31	8	O	2.518	–3.504	1.478
32	8	O	0.367	–4.028	–0.342
33	8	O	–5.790	2.386	1.854
34	1	H	–0.247	1.899	–0.843

Appendix 2: Optimized Cartesian coordinates (in Å) of atoms in compound B

No	Atomic number	Atomic type	X	Y	Z
1	6	C	–2.417	0.023	-0.139
2	7	N	-3.344	-0.896	-0.091
3	7	N	-2.742	-2.115	-0.336
4	6	C	-1.463	-1.910	-0.512
5	7	N	-1.194	-0.564	-0.389
6	7	N	-0.009	0.131	-0.593
7	7	N	0.943	-0.455	0.351
8	7	N	2.141	0.253	0.260
9	6	C	2.401	1.601	0.287
10	7	N	3.685	1.809	0.135
11	7	N	4.303	0.583	0.022
12	6	C	3.372	-0.335	0.089
13	1	H	-0.705	-2.647	-0.733
14	1	H	1.633	2.353	0.395
15	6	C	3.589	-1.800	0.046
16	7	N	3.294	-2.522	1.389
17	7	N	2.682	–2.458	–1.029
18	7	N	5.075	-2.121	-0.272
19	8	O	5.833	-1.833	0.630
20	8	O	5.319	-2.623	-1.349
21	8	O	2.744	-1.935	-2.121
22	8	O	1.993	-3.403	-0.678
23	8	O	2.578	-1.924	2.177
24	6	C	-2.614	1.475	0.071
25	7	N	-2.005	2.008	1.393
26	7	N	-1.955	2.307	-1.070
27	7	N	-4.126	1.815	0.108
28	8	O	-4.562	2.449	-0.831
29	8	O	-4.702	1.400	1.092
30	8	O	-2.084	1.827	-2.178
31	8	O	-1.400	3.340	-0.745
32	8	O	-1.011	1.411	1.796
33	8	O	-2.532	2.978	1.886
34	8	O	3.793	-3.620	1.517
35	9	F	0.479	-0.324	-1.845
36	1	H	0.523	-0.279	1.267

Appendix 3: Optimized Cartesian coordinates (in Å) of atoms in compound C

No	Atomic number	Atomic type	X	Y	Z
1	6	C	–3.095	–0.095	–0.047
2	7	N	–4.051	–0.978	–0.126
3	7	N	–3.474	–2.232	–0.248
4	6	C	–2.190	–2.059	–0.234
5	7	N	–1.857	–0.720	–0.109
6	7	N	–0.679	–0.018	–0.105
7	7	N	0.325	–0.756	–0.091
8	7	N	1.484	–0.035	–0.115
9	6	C	1.744	1.318	–0.243
10	7	N	3.034	1.515	–0.261
11	7	N	3.662	0.285	–0.141
12	6	C	2.734	–0.627	–0.057
13	6	C	2.967	–2.087	0.075
14	7	N	2.137	–2.884	–0.972
15	7	N	2.606	–2.654	1.471
16	7	N	4.465	–2.410	–0.161
17	8	O	4.741	–2.985	–1.195
18	8	O	5.198	–2.044	0.733
19	8	O	1.772	–2.015	2.095
20	8	O	3.162	–3.682	1.791
21	8	O	1.682	–3.954	–0.622
22	8	O	2.045	–2.338	–2.057
23	6	C	–3.278	1.372	0.083
24	7	N	–2.403	2.125	–0.956
25	7	N	–2.901	1.928	1.480
26	7	N	–4.762	1.754	–0.154
27	8	O	–5.509	1.391	0.730
28	8	O	–5.014	2.366	–1.172
29	8	O	–2.099	1.258	2.111
30	8	O	–3.416	2.981	1.792
31	8	O	–1.804	3.112	–0.571
32	8	O	–2.409	1.629	–2.067
33	9	F	–1.280	–2.987	–0.334
34	1	H	0.972	2.068	–0.321

Appendix 4: Optimized Cartesian coordinates (in Å) of atoms in compound D

No	Atomic number	Atomic type	X	Y	Z
1	6	C	–2.529	1.180	–0.443
2	7	N	–3.417	0.341	–0.897
3	7	N	–2.855	–0.925	–0.880
4	6	C	–1.639	–0.823	–0.420
5	7	N	–1.364	0.500	–0.134
6	7	N	–0.232	1.089	0.381
7	7	N	0.926	0.499	–0.381
8	7	N	2.059	1.089	0.133
9	6	C	2.334	2.412	0.419
10	7	N	3.549	2.514	0.879
11	7	N	4.112	1.248	0.896
12	6	C	3.224	0.409	0.442
13	6	C	–2.715	2.646	–0.287
14	7	N	–1.546	3.415	–0.954
15	7	N	–4.053	3.096	–0.934
16	7	N	–2.783	3.113	1.190
17	8	O	–2.271	2.362	2.004
18	8	O	–3.315	4.187	1.381
19	8	O	–3.982	3.789	–1.928
20	8	O	–5.035	2.700	–0.341
21	8	O	–1.288	3.050	–2.084
22	8	O	–0.994	4.278	–0.294
23	6	C	3.410	–1.057	0.287
24	7	N	2.240	–1.825	0.955
25	7	N	3.477	–1.525	–1.190
26	7	N	4.748	–1.507	0.934
27	8	O	4.678	–2.199	1.928
28	8	O	5.729	–1.111	0.340
29	8	O	4.008	–2.599	–1.379
30	8	O	2.966	–0.774	–2.004
31	8	O	1.688	–2.689	0.296
32	8	O	1.984	–1.460	2.085
33	1	H	–0.927	–1.623	–0.274
34	1	H	1.622	3.212	0.273
35	9	F	–0.015	0.491	1.644
36	9	F	0.710	1.097	–1.644

Appendix 5: Optimized Cartesian coordinates (in Å) of atoms in compound E

No	Atomic number	Atomic type	X	Y	Z
1	6	C	–3.309	1.257	0.659
2	7	N	–4.162	0.563	1.358
3	7	N	–3.520	–0.575	1.822
4	6	C	–2.302	–0.534	1.390
5	7	N	–2.077	0.617	0.634
6	7	N	–1.014	1.102	–0.079
7	7	N	0.019	0.423	0.079
8	7	N	1.083	0.908	–0.633
9	6	C	1.308	2.049	–1.389
10	7	N	2.526	2.100	–1.822
11	7	N	3.167	0.962	–1.358
12	6	C	2.314	0.268	–0.659
13	6	C	2.603	–1.020	0.019
14	7	N	1.911	–2.241	–0.637
15	7	N	4.127	–1.303	–0.010
16	7	N	2.152	–0.982	1.508
17	8	O	1.695	–2.004	1.976
18	8	O	2.326	0.093	2.053
19	8	O	4.556	–1.594	–1.107
20	8	O	4.718	–1.207	1.047
21	8	O	0.900	–1.989	–1.274
22	8	O	2.425	–3.320	–0.435
23	6	C	–3.598	2.545	–0.019
24	7	N	–3.147	2.506	–1.508
25	7	N	–2.907	3.766	0.637
26	7	N	–5.122	2.828	0.009
27	8	O	–5.551	3.118	1.107
28	8	O	–5.713	2.730	–1.048
29	8	O	–1.896	3.514	1.275
30	8	O	–3.420	4.845	0.434
31	8	O	–3.320	1.431	–2.053
32	8	O	–2.690	3.529	–1.977
33	9	F	–1.364	–1.405	1.599
34	9	F	0.369	2.930	–1.598

Appendix 6: Optimized Cartesian coordinates (in Å) of atoms in compound F

No	Atomic number	Atomic type	X	Y	Z
1	6	C	–2.564	0.812	–0.468
2	7	N	–3.556	0.258	–1.107
3	7	N	–3.203	–1.038	–1.444
4	6	C	–2.009	–1.228	–0.983
5	7	N	–1.515	–0.094	–0.364
6	7	N	–0.351	0.114	0.341
7	7	N	1.933	–0.059	0.151
8	6	C	2.30	1.163	0.676
9	7	N	3.512	1.074	1.168
10	7	N	3.966	–0.218	0.962
11	6	C	3.029	–0.882	0.346
12	6	C	3.115	–2.304	–0.073
13	7	N	1.892	–3.112	0.438
14	7	N	4.404	–2.954	0.500
15	7	N	3.187	–2.498	–1.608
16	8	O	2.734	–1.583	–2.276
17	8	O	3.663	–3.547	–1.990
18	8	O	4.260	–3.789	1.369
19	8	O	5.427	–2.544	–0.009
20	8	O	1.371	–3.891	–0.337
21	8	O	1.586	–2.869	1.591
22	6	C	–2.607	2.165	0.143
23	7	N	–4.047	2.731	0.049
24	7	N	–1.660	3.206	–0.499
25	7	N	–2.221	2.111	1.653
26	8	O	–1.664	3.090	2.108
27	8	O	–2.544	1.085	2.222
28	8	O	–2.020	4.362	–0.475
29	8	O	–0.612	2.748	–0.933
30	8	O	–4.664	2.810	1.093
31	8	O	–4.391	3.033	–1.074
32	9	F	–1.297	–2.314	–1.068
33	1	H	1.672	2.034	0.659
34	9	F	–0.347	–0.843	1.382
35	7	N	0.779	–0.432	–0.500
36	9	F	0.685	0.389	–1.644

Appendix 7: Optimized Cartesian coordinates (in Å) of atoms in compound G

No	Atomic number	Atomic type	X	Y	Z
1	6	C	–2.576	0.297	–0.472
2	7	N	–3.557	–0.359	–1.023
3	7	N	–3.444	–1.697	–0.688
4	6	C	–2.410	–1.802	0.079
5	7	N	–1.771	–0.584	0.250
6	7	N	–0.734	–0.191	1.069
7	7	N	0.357	–1.097	0.959
8	7	N	1.541	–0.465	1.280
9	6	C	1.880	0.444	2.267
10	7	N	3.125	0.782	2.201
11	7	N	3.679	0.057	1.159
12	6	C	2.751	–0.678	0.619
13	9	F	–1.945	–2.895	0.611
14	9	F	0.993	0.904	3.104
15	6	C	–2.442	1.776	–0.526
16	7	N	–1.178	2.301	–1.238
17	7	N	–3.664	2.371	–1.280
18	7	N	–2.435	2.392	0.906
19	8	O	–1.783	3.403	1.067
20	8	O	–3.115	1.787	1.714
21	8	O	–3.665	2.153	–2.473
22	8	O	–4.469	2.983	–0.607
23	8	O	–0.205	1.566	–1.173
24	8	O	–1.262	3.395	–1.753
25	6	C	2.984	–1.647	–0.486
26	7	N	1.873	–1.568	–1.558
27	7	N	3.058	–3.120	–0.007
28	7	N	4.355	–1.354	–1.169
29	8	O	4.323	–0.877	–2.284
30	8	O	5.313	–1.653	–0.488
31	8	O	3.622	–3.894	–0.750
32	8	O	2.514	–3.348	1.061
33	8	O	1.402	–2.616	–1.957
34	8	O	1.589	–0.433	–1.892
35	9	F	–1.230	–0.247	2.399
36	9	F	0.169	–2.130	1.912

Appendix 8: Molecular energy components

Species	E	ZPVE	H_T	$\Delta_{sub}H°(298)$
A	–1898.72685	453.879	75.1455	191.8798
B	–1999.13126	493.014	78.5455	195.5762
C	–1997.98140	432.735	77.4948	191.3728
D	–2098.31985	466.122	81.0751	191.3377
E	–2097.23606	411.533	79.8979	191.4136
F	–2197.57926	445.445	83.3308	194.0202
G	–2296.83232	424.258	85.5844	195.0366

Note: E is total electronic energy in atomic units, ZPVE is zero-point vibrational energy in kJ mol^{-1}, H_T is thermal correction to enthalpy in kJ mol^{-1}, $\Delta_{sub}H°(298)$ is the enthalpy of sublimation in kJ mol^{-1}.

Appendix 9: Molecular surface properties used in equations (15), (17) and (23)

Species	υ	σ^2_{tot}	A	V
A	0.1435	191.54	358.12	392.34
B	0.1549	217.87	357.86	403.38
C	0.1312	180.60	360.72	395.89
D	0.1621	154.83	359.46	408.91
E	0.1190	168.19	364.12	399.54
F	0.1465	150.93	365.38	412.57
G	0.1307	135.08	370.82	415.63

Note: υ is the degree of balance between the positive and the negative potentials on a molecular surface (unitless), σ^2_{tot} is an indicator of the variability of electrostatic potential in $(\text{kcal mol}^{-1})^2$, A is the molecular surface area for the structures in $Å^2$, V is the volume enclosed by the 0.001 atomic unit contour of electron density of the molecule in $Å^3$.

Appendix 10: Enthalpies of formation of solid compounds, all values in kJ mol^{-1}

	Equation of chemical reaction	$\Delta_f H°$(c, 298)
A1	$C_6H_2N_{14}O_{12} = CO + 5CO_2 + 7N_2 + H_2O$	903.41
A2	$C_6H_2N_{14}O_{12} = 0.5C + 5.5CO_2 + 7N_2 + H_2O$	832.66
A3	$C_6H_2N_{14}O_{12} = 6CO + 7N_2 + H_2O + 2.5O_2$	906.11
A4	$C_6H_2N_{14}O_{12} = 5CO + C + 7N_2 + H_2O + 3O_2$	765.16
A5	$C_6H_2N_{14}O_{12} + 0.5O_2 = 6CO_2 + 7N_2 + H_2O$	902.87
	Average $\Delta_f H°$(A, c)	**862±62**
B1	$C_6H_3N_{14}O_{12}F = CO + 5CO_2 + 7N_2 + H_2O + HF$	851.01
B2	$C_6H_3N_{14}O_{12}F = 0.5C + 5.5CO_2 + 7N_2 + H_2O + HF$	784.47
B3	$C_6H_3N_{14}O_{12}F = 6CO + 7N_2 + H_2O + 2.5O_2 + HF$	853.71
B4	$C_6H_3N_{14}O_{12}F = 5CO + C + 7N_2 + H_2O + 3O_2 + HF$	712.76
B5	$C_6H_3N_{14}O_{12}F + 0.5O_2 = 6CO_2 + 7N_2 + H_2O + HF$	855.06
	Average $\Delta_f H°$(B, c)	**811±63**
C1	$C_6H_1N_{14}O_{12}F = 0.5CO + 5.5CO_2 + 7N_2 + 0.5H_2O + 0.5F_2$	751.47
C2	$C_6H_1N_{14}O_{12}F = 6CO_2 + 7N_2 + HF$	755.65
C3	$C_6H_1N_{14}O_{12}F = 6CO + 7N_2 + 3O_2 + HF$	758.89
C4	$C_6H_1N_{14}O_{12}F = 5CO + C + 7N_2 + 0.5H_2O + 3.25O_2 + 0.5F_2$	609.28
C5	$C_6H_1N_{14}O_{12}F + 0.25O_2 = 6CO_2 + 7N_2 + 0.5\ H_2O + 0.5F_2$	742.57
	Average $\Delta_f H°$(C, c)	**724±64**
D1	$C_6H_2N_{14}O_{12}F_2 = 6CO_2 + 7N_2 + 2HF$	874.25
D2	$C_6H_2N_{14}O_{12}F_2 = 0.5C + 5.5CO_2 + 7N_2 + H_2O + F_2$	790.93
D3	$C_6H_2N_{14}O_{12}F_2 = 6CO + 7N_2 + 3O_2 + HF$	877.49
D4	$C_6H_2N_{14}O_{12}F_2 = 5CO + C + 7N_2 + 3.5O_2 + 2HF$	736.54
D5	$C_6H_2N_{14}O_{12}F_2 + 0.5O_2 = 6CO_2 + 7N_2 + H_2O + F_2$	861.51
	Average $\Delta_f H°$(D, c)	**828±62**
E1	$C_6N_{14}O_{12}F_2 = 6CO_2 + 7N_2 + F_2$	594.75
E2	$C_6N_{14}O_{12}F_2 = 0.5C + 5.5CO_2 + 7N_2 + 0.5O_2 + F_2$	524.16
E3	$C_6N_{14}O_{12}F_2 = 6CO + 7N_2 + 3O_2 + F_2$	593.40
E4	$C_6N_{14}O_{12}F_2 = 5CO + C + 7N_2 + 3.5O_2 + F_2$	452.45
E5	$C_6N_{14}O_{12}F_2 + 0.5O_2 = 6CO_2 + 7N_2 + F_2O$	589.36
	Average $\Delta_f H°$(E, c)	**551±63**
F1	$C_6H_1N_{14}O_{12}F_3 = 0.5CO + 5.5CO_2 + 7N_2 + 0.5H_2O + 1.5F_2$	600.08
F2	$C_6H_1N_{14}O_{12}F_3 = 6CO_2 + 7N_2 + HF + F_2$	694.30
F3	$C_6H_1N_{14}O_{12}F_3 = 6CO + 7N_2 + 3O_2 + HF + F_2$	697.55
F4	$C_6H_1N_{14}O_{12}F_3 = 5CO + C + 7N_2 + 0.5H_2O + 3.25O_2 + 1.5F_2$	547.94

	Equation of chemical reaction	$\Delta_f H°$(c, 298)
F5	$C_6H_1N_{14}O_{12}F_3 + 0.25O_2 = 6CO_2 + 7N_2 + 0.5\ H_2O + 1.5F_2$	575.84
	Average $\Delta_f H°$(F, c)	**623±69**
G1	$C_6N_{14}O_{12}F_4 = 6CO_2 + 7N_2 + 2F_2$	536.81
G2	$C_6N_{14}O_{12}F_4 = 0.5C + 5.5CO_2 + 7N_2 + 0.5O_2 + 2F_2$	466.23
G3	$C_6N_{14}O_{12}F_4 = 6CO + 7N_2 + 3O_2 + 2F_2$	535.46
G4	$C_6N_{14}O_{12}F_4 = 5CO + C + 7N_2 + 3.5O_2 + 2F_2$	394.51
G5	$C_6N_{14}O_{12}F_4 + O_2 = 6CO_2 + 7N_2 + 2F_2O$	526.03
	Average $\Delta_f H°$(G, c)	**492±62**

Appendix 11: Molecular structures of the reference compounds used for energetic properties comparison in Table 7

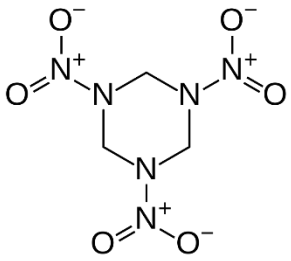

RDX[a]

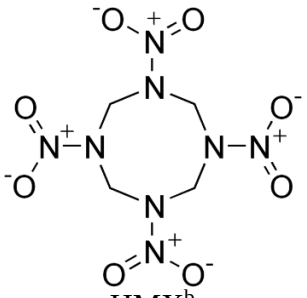

HMX[b]

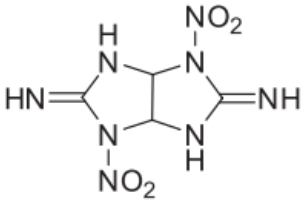

$C_4H_6N_8O_4$[c]

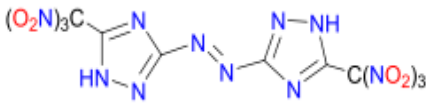

$C_6H_2N_{14}O_{12}$[d]

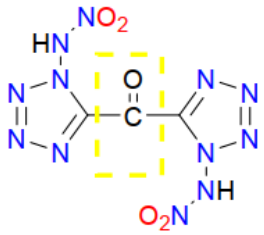

$C_3H_2N_{12}O_5$[e]

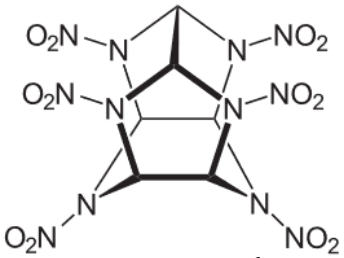

$C_6H_6N_{12}O_{12}$[f]

[a] Byrd and Rice (2006), Mei *et al*. (2019), Zhang *et al*. (2019)

[b] Mei *et al*. (2019), Zhang *et al*. (2019), Rice *et al*. (1999)

[c] Jin *et al*. (2014)

[d] Zhang *et al*. (2019)

[e] Mei *et al*. (2019)

[f] Politzer and Murray (2011)

RESEARCH OUTPUT

(i) Publication

Ansbert, C., Pogrebnoi, A., & Pogrebnaya, T. (2020). High energy density materials based on fluorinated bridged trinitromethyl azo triazole derivatives: A quantum chemical study of thermodynamic and energetic properties. *Springer Nature Applied Sciences*, *2*(11), 1-13.

(ii) Poster on High energy density materials based on fluorinated bridged trinitromethyl azo triazole derivatives: A quantum chemical study of thermodynamic and energetic properties.